Weak-anisotropy moveout approximations for P waves in homogeneous layers of monoclinic or higher anisotropy symmetries

Véronique Farra [1)], Ivan Pšenčík [2)] and Petr Jílek [3)]

[1)]Institut de Physique du Globe de Paris, Sorbonne Paris Cité, UMR 7154 CNRS, France. E-mail: farra@ipgp.fr
[2)]Institute of Geophysics, Acad. Sci. of Czech Republic, Boční II, 141 31 Praha 4, Czech Republic. E-mail: ip@ig.cas.cz
[3)]BP Upstream Technology, 501 Westlake Park Blvd, Houston, TX 77079-2604. E-mail: petr.jilek@bp.com

Abstract

We use the so-called WA parameterization as an alternative to the parameterization of generally anisotropic media by stiffness tensor. WA parameters have important advantages. They consist of linear combinations of normalized stiffness tensor elements controlling various seismic signatures, hence they are theoretically extractable from seismic data. They are dimensionless and of the same order of magnitude. WA parameters have a clear physical interpretation, similarly to Thomsen-type parameterizations, however, they are applicable to anisotropy of arbitrary symmetry and strength. They are defined in coordinate systems independent of symmetry elements of studied media. Expressions using WA parameters naturally simplify as the anisotropy becomes weaker or anisotropy symmetry increases. We argue that, due to these useful properties, WA parameterization is well-suited for solving forward and inverse problems, and can potentially provide a framework for seismic data processing in generally anisotropic media.

Using the *WA parameterization*, we derive and test approximate P-wave moveout formulae for anisotropic media up-to monoclinic symmetry underlaid by a horizontal reflector coinciding with a symmetry plane. Derived traveltime formulae represent an expansion of the traveltime with respect to (small) WA parameters. We express the moveout formulae in the common form of non-hyperbolic moveout, containing normal moveout velocity and a quartic coefficient as functions of WA parameters. All the resulting formulae are simple, transparent, and described by only a few WA parameters. The accuracy of the formulae depends strongly on the deviation of ray- and phase-velocity directions, which is more pronounced for strongly anisotropic media. The errors do not generally increase with increasing offset, neither they increase with decreasing anisotropy symmetry. The accuracy of our formulae is comparable to, or better than, the accuracy of commonly used formulae. For anisotropy with a non-negligible strength of 25%, the relative traveltime errors do not exceed 1%.

Seismic Waves in Complex 3–D Structures, **25** (2015), 51–88 (ISSN 2336–3827, online at http://sw3d.cz)

Introduction

Motivation

Reflection moveout has been extensively studied and discussed in literature in the past. The reason is simple: as a fundamental seismic attribute directly measured from reflection seismic data with a high degree of accuracy, reflection moveout offers a primary link between the measured reflection traveltimes on one side and the properties of the Earth (i.e., velocity, anisotropy) on the other. The reflection moveout equation thus provides a theoretical basis for seismic data processing in time-domain (for recent advances in time-domain data processing, see Fomel, 2014) and, in some form or another, moveout quantities are often embedded in depth-domain data processing workflows as well.

Moveout equations evolved significantly over the time to accommodate increasing complexities of the subsurface such as anisotropy and heterogeneity. Corresponding approximations have also been developed, providing important analytical insight, exposing first-hand information about the subsurface potentially extractable from the measured moveout attributes. Complementary approaches have been introduced to additionally remove the limiting assumption of laterally homogeneous medium behind most moveout formulae (Li and Fomel, 2013), expanding the applicability of the time-domain data processing to more complex subsurface settings. One may ask at this point if there is anything more we can possibly do regarding the reflection moveout to make further meaningful theoretical advances.

There is one good reason suggesting we perhaps should: increasing resolution power of multi-azimuth, long-offset seismic data acquired today opens a possibility (and a need) to account for lower anisotropy symmetries in data processing flows. In fact, at some point, one should be ready to handle arbitrary anisotropy, which includes generally tilted TI or orthorhombic symmetries. At the same time, however, we should not lose the view of important anisotropy parameters that drive the processes, and we should seek ways to simplify modeling and inversion problems as much as possible. Clearly, suitable approximations of various seismic attributes have their place in seismic data processing, especially when advancing towards more general anisotropy symmetries. Reflection moveout is not an exception.

Influence of anisotropy on reflection moveout using approximations was studied, for example, by Tsvankin and Thomsen (1994), Sayers and Ebrom (1997), or Tsvankin (1997). Among the first contributions beyond orthorhombic symmetry was the presentation by Pšenčík and Gajevski (1998) who derived, among other quantities, a weak-anisotropy approximation for NMO velocity valid for arbitrary anisotropic media. An alternative approximation was also derived by Rasolofosaon (2000). Undoubtedly, the inversion of normal moveout for monoclinic media by Grechka et al. (2000) pushed the limits not only in terms of the theoretical development but also practical applications.

Exploring lower anisotropy symmetries, however, comes with a price: the corresponding expressions usually become either too complex, providing no analytic insight, or their (simplifying) approximations lose required accuracy. In either case, the information about the subsurface becomes more obscured and thus more difficult to extract from data. In this paper we attempt to alleviate some of the difficulties by offering accurate approx-

imations suitable for modeling and inversion of reflection moveout in media with lower anisotropy symmetries.

The key to a successful generalization for arbitrary anisotropy is a proper choice of medium parameterization. Such a parameterization should be universally applicable regardless of the anisotropy strength, symmetry, and its orientation in a chosen coordinate system. It should promote an easy manipulation with seismic quantities, offering analytic insight, and naturally resulting in simplifications of corresponding expressions when anisotropy becomes weak or anisotropy symmetry increases. Importantly, the medium parameters should also be naturally constrained by seismic data. In other words, inversion for such parameters from measurable seismic attributes should be realistically possible, depending, of course, on data coverage and noise contamination.

In our derivations of reflection moveout outlined in the next section, we use what we refer to as *weak anisotropy* (WA) parameterization (Mensch and Rasolofosaon, 1997; Pšenčík and Gajewski, 1998) that possess the desirable properties specified above. (As explained later in the text, the name *weak anisotropy* is misleading - a complete set of WA parameters fully describes anisotropic medium of arbitrary symmetry and strength, as stiffness tensor does.) In some respect, WA parameterization resembles well-known Thomsen parameterization (Thomsen, 1986; Tsvankin, 1997), preserving its advantages previously discussed in literature. Unlike Thomsen, however, WA parameters are applicable to general anisotropy. Moreover, they are dimensionless and of a comparable magnitude, which offers a significant advantage in inversion problems. As showed on the case of moveout formulae in this paper, WA parameters are also very useful in weak-anisotropy approximations, resulting in simplified expressions, preserving reasonable accuracy of approximations even if the weak-anisotropy assumption is clearly violated. Other important advantages of WA parameterization are discussed in the main text below.

Finally, it should be emphasized that the utilization of WA parameters described in this paper is not limited to weak anisotropy approximations of reflection moveout. WA parameters can be used to parameterize any seismic quantity describing P- or S-wave propagation in anisotropic media of arbitrary anisotropy symmetry and strength. In fact, because the WA parameters are designed to explain data signatures, the WA parameterization could provide a more natural framework for seismic data processing in generally anisotropic media in future, including migrations, tomography, or FWI. Clearly, once the WA parameterization is implemented in a processing algorithm, the algorithm is universally applicable without a necessity for further modifications every time anisotropy symmetry changes. Let us mention that other parameterizations of anisotropic media are also possible, see, e.g., Chen and Tromp (2007).

Method

The moveout formulae are often derived as expansions of the square of reflection traveltime T into a Taylor series in terms of the square of the source-receiver offset x, see e.g., Thomsen (1986), Tsvankin and Thomsen (1994), Alkhalifah and Tsvankin (1995), Tsvankin (2001), Stovas (2010), Tsvankin and Grechka (2011). An expansion of the inverse-squared ray velocity in spherical harmonics has also been used, see Sayers and Ebrom (1997). As a consequence, the resulting moveout formulae are accurate at small and moderate offsets but lose their accuracy as offsets increase. Empirical corrections

are often added to the original expressions to guarantee a good behavior at some large offset (usually infinity). However, the accuracy for other large offsets is less predictable, especially for low anisotropy symmetries.

We propose an alternative way to derive reflection moveout formulae, based on *weak-anisotropy (WA)* approximation. In this approach, we expand T^2 in terms of WA parameters (discussed in detail below), which describe anisotropy as a departure from a known isotropic background. In the WA approximation, the departure is assumed to be small, resulting in small WA parameters. As we demonstrate below, the accuracy of such WA moveout formulae does not deteriorate with increasing offset, neither it becomes compromised with decreasing anisotropy symmetry. The accuracy is determined by the strength of anisotropy. However, we show that even for anisotropy stronger than 20%, which cannot be considered weak, the accuracy of moveout formulae is still fairly good. Additionally, we also show how the accuracy can be further improved by adding higher-order terms, if desirable, which is a relatively simple process in our WA approach.

The WA approach has another clear advantage. The first-order WA approximation results in a full separation of P waves from S waves. WA formulae can thus be derived and used for P- and S-waves separately without any cross-contamination. This advantage holds in general and goes beyond expressions for reflection moveout. One consequence also is that the number of WA parameters required to describe P waves reduces to 15 in the most general case of triclinic anisotropy as opposed to 21 when stiffness tensor parameterization is used.

We used the weak-anisotropy approach previously to derive moveout formulae for unconverted reflected P and S waves for transversely isotropic media with the vertical axis of symmetry (VTI), and for the so-called dip-constrained transversely isotropic (DTI) media, see Farra and Pšenčík (2013a,b), respectively. In both cases, rays were situated in the plane containing TI symmetry axis. In this paper we concentrate on the situations, in which down-going and up-going rays of the reflected wave are situated in a plane perpendicular to the reflector, and are symmetrical with respect to the normal to this reflector (Farra and Pšenčík, 2014). Such situations occur everywhere, where the reflector coincides with a symmetry plane of the considered anisotropic medium. Such media include transversely isotropic media with vertical (VTI) or horizontal (HTI) axis of symmetry, orthorhombic media with one of the symmetry planes coinciding with the reflector, and even monoclinic media, whose plane of symmetry coincides with the reflector. We perform the derivation in two steps. In the first step, we derive the moveout formulae in terms of local (primed) WA parameters in the plane (x_1', x_3') of a local (primed) Cartesian coordinate system containing the source-receiver line. In the second step, we express the involved local WA parameters in terms of non-primed WA parameters in global Cartesian coordinate system. Both coordinate systems share the same vertical axis, their horizontal axes making an azimuth angle. For expressing the local WA parameters in terms of global ones, we use the transformation relations of WA parameters between the two coordinate systems. In this way, we obtain azimuthally-dependent reflection moveout formulae in global coordinates.

Outline

The paper is organized as follows. We start with a detail review of WA parameterization. Then we introduce the exact moveout expression for an unconverted P-wave reflected from a plane reflector parallel to the plane of symmetry of the overlaying anisotropic medium. As a next key step, we present three WA approximations of the ray (group) velocity that differ in their accuracy, including one *second-order* WA approximation. We use these expressions to derive three approximations of the reflection moveout. For easy evaluation, we rearrange the moveout formulae into the common form of non-hyperbolic moveout, containing normal moveout velocity and a quartic coefficient expressed in terms of WA parameters. We study accuracy of the derived formulae using three examples of anisotropic media: HTI, orthorhombic and monoclinic. We compare the approximate results with traveltimes obtained from an exact ray tracer. For the orthorhombic medium, we also compare our results with those of Tsvankin and Grechka (2011) as a reference. Finally, Appendices A, B, and C include further details that allow the reader to fully reproduce the presented derivations and results.

Throughout the text, the lower-case indices $i, j, k, l, ...$ take the values of 1,2,3, the upper-case indices $I, J, K, L, ...$ take the values of 1,2. The Einstein summation convention over repeated indices applies. In order to distinguish Thomsen (1986) from WA parameters, the superscript T is used over the Thomsen's parameters.

WA parameters

In all our derivations of weak-anisotropy formulae, including, for example, formulae for eigenvalues and eigenvectors of the Christoffel matrix, phase and ray velocities, polarization vectors, ray tracing and dynamic ray tracing, reflection/transmission coefficients, source-directivity functions, etc., we use a perturbation theory, in which anisotropy is considered as a perturbation from an isotropic background, so-called *weak-anisotropy approximation*. Detailed derivation of some of the weak-anisotropy formulae for the above-mentioned attributes can be found, for example, in Farra and Pšenčík (2003) for P and S waves, Pšenčík and Gajewski (1998), Pšenčík and Farra (2005, 2007) for P waves and Farra and Pšenčík (2008, 2010) for coupled S waves. Many other useful references can be found in the above publications as well.

For a convenient parameterization of seismic attributes in weak-anisotropy approximation, we use 21 so-called weak-anisotropy (WA) parameters (slightly modified parameters originally introduced by Mensch and Rasolofosaon, 1997). We adopted the term *weak-anisotropy parameters* since we often use them in applications related to weak anisotropy. However, it must be emphasized here that the WA parameters can be used for description of *anisotropy of any type and strength*. In fact, the WA parameters represent an alternative set to the full set of 21 elastic parameters $C_{\alpha\beta}$ or density-normalized elastic parameters $A_{\alpha\beta}$ in the Voigt notation. Some advantages of the WA parameterization are discussed below.

All 21 WA parameters can be expressed in terms of 21 density-normalized elastic parameters $A_{\alpha\beta}$ and two constant reference P- and S-wave velocities α_0 and β_0 in the following way:

$$\epsilon_x = \frac{A_{11} - \alpha_0^2}{2\alpha_0^2} \ , \quad \epsilon_y = \frac{A_{22} - \alpha_0^2}{2\alpha_0^2} \ , \quad \epsilon_z = \frac{A_{33} - \alpha_0^2}{2\alpha_0^2} \ ,$$

$$\delta_x = \frac{A_{23} + 2A_{44} - \alpha_0^2}{\alpha_0^2} \ , \quad \delta_y = \frac{A_{13} + 2A_{55} - \alpha_0^2}{\alpha_0^2} \ , \quad \delta_z = \frac{A_{12} + 2A_{66} - \alpha_0^2}{\alpha_0^2} \ ,$$

$$\chi_x = \frac{A_{14} + 2A_{56}}{\alpha_0^2} \ , \quad \chi_y = \frac{A_{25} + 2A_{46}}{\alpha_0^2} \ , \quad \chi_z = \frac{A_{36} + 2A_{45}}{\alpha_0^2} \ ,$$

$$\epsilon_{15} = \frac{A_{15}}{\alpha_0^2} \ , \quad \epsilon_{16} = \frac{A_{16}}{\alpha_0^2} \ , \quad \epsilon_{24} = \frac{A_{24}}{\alpha_0^2} \ , \quad \epsilon_{26} = \frac{A_{26}}{\alpha_0^2} \ , \quad \epsilon_{34} = \frac{A_{34}}{\alpha_0^2} \ , \quad \epsilon_{35} = \frac{A_{35}}{\alpha_0^2} \ ,$$

$$\epsilon_{46} = \frac{A_{46}}{\alpha_0^2} \ , \quad \epsilon_{56} = \frac{A_{56}}{\alpha_0^2} \ , \quad \epsilon_{45} = \frac{A_{45}}{\beta_0^2} \ ,$$

$$\gamma_x = \frac{A_{44} - \beta_0^2}{2\beta_0^2} \ , \quad \gamma_y = \frac{A_{55} - \beta_0^2}{2\beta_0^2} \ , \quad \gamma_z = \frac{A_{66} - \beta_0^2}{2\beta_0^2} \ . \qquad (1)$$

The velocities α_0 and β_0 can be considered as velocities of a reference isotropic background medium. They can be chosen arbitrarily without any loss of generality and accuracy of expressions parameterized by WA parameters from equations (1) above. Of course, the magnitudes of WA parameters depend on the choice of α_0 and β_0. Many seismic attributes are, however, independent of the choice of α_0 and β_0. Their choice can be therefore tuned for a particular application. More discussion on the choice of α_0 and β_0 follows below.

The WA parameters in equations (1) can be viewed as a generalization of Thomsen's (1986) parameters introduced for VTI media. In the following we make some basic comparisons of the two.

First of all, unlike Thomsen's (1986) parameters, WA parameters can be used for description of any anisotropy symmetry. That, of course, includes higher symmetries with inclined symmetry planes or axes, such as tilted TI or tilted orthorhombic media.

From the theoretical standpoint, all WA parameters are related *linearly* to density-normalized elastic parameters $A_{\alpha\beta}$. This makes the transformation from WA parameters to $A_{\alpha\beta}$ and vice versa an elementary task, which may be an important advantage for theoretical development as well as practical use. Such a transformation of Thomsen's VTI parameters is complicated by nonlinearity of Thomsen's δ^T (the superscript T is used to denote Thomsen anisotropy parameters) in $C_{\alpha\beta}$ or $A_{\alpha\beta}$. Another important consequence of linear relation of WA and density-normalized elastic parameters is the simple possibility of transforming WA parameters from one coordinate system to another. This is impossible with Thomsen's parameters and their generalizations because they are defined in coordinate systems firmly fixed to the symmetry elements of the considered media.

Please, note that the definitions of parameters δ_x and δ_y, and γ_x, and γ_y in equation (1) above are interchanged in Pšenčík and Gajewski (1998, eq.(17b)), Farra and Pšenčík (2003, eq. (A3)) and Pšenčík and Farra (2005, eq.(A-1); 2007, eq.(A1)).

For the choice $\alpha_0^2 = A_{33}$ and $\beta_0^2 = A_{44}$, VTI WA parameters ϵ_x and γ_z from equations (1) correspond exactly to Thomsen's ϵ^T and γ^T. Parameter δ_y is a linearized version of Thomsen's δ^T in that case. In fact, Thomsen's δ^T can be expressed exactly in terms of WA parameter δ_y, $\delta^T = \delta_y + 1/2\delta_y^2(1-r^2)^{-1}$, the factor r being the ratio of β_0 and α_0, $r = \beta_0/\alpha_0$. The above described relations of Thomsen's and WA parameters also hold for extensions of Thomsen's specification to HTI and orthorhombic media (Tsvankin, 1997) or monoclinic media (Grechka et al., 2000).

Another difference between the WA and Thomsen's (1986) parameterizations is the presence of an arbitrary background non-zero constant velocities α_0 and β_0 in WA parameters, replacing the P- and S-wave velocities $\sqrt{A_{33}}$ and $\sqrt{A_{55}}$ along the axis of symmetry used by Thomsen (1986). The use of α_0 and β_0 makes the applications of WA parameters more flexible and accurate. For example, when a cross-hole experiment is considered, in which waves propagate prevailingly horizontally (and not vertically as in Thomsen's original design), α_0 and β_0 can be chosen as velocities corresponding to the horizontal propagation. In short-offset reflection or migration applications, on the other hand, it is better to choose α_0 and β_0 the same way as Thomsen (1986), i.e., as vertical velocities.

Flexible choice of α_0 and β_0 is especially useful in practical linearized inversions, when magnitudes of anisotropic updates are required to be small for the inversion to be accurate. The magnitudes of WA parameters can be a priori optimized for a given inversion (i.e., making the magnitudes as small as possible) by a meaningful choice of the α_0 and β_0 velocities: they can be chosen such that the resulting isotropic background medium is, on average, as close to the actual anisotropic medium as practically possible for a given experiment. Note that, in practice, such α_0 and β_0 estimates could be obtained, for example, from the corresponding isotropic inversion preceding the inversion for WA parameters.

It is important to add at this point that although WA parameters themselves depend on the choice of the velocities α_0 and β_0, the formulae for the weak-anisotropy P- and S-wave eigenvalues and eigenvectors of the Christoffel matrix and for weak-anisotropy phase and ray velocities and polarization vectors are *independent* of α_0 and β_0 (Farra and Pšenčík, 2003).

Another non-negligible advantage of WA parameterization over Thomsen (1986) becomes apparent when solving linear and non-linear anisotropic inversion problems (note that WA parameterization usage is limited to neither weak anisotropy nor linear inversions). The advantage resides in the fact that all 21 WA parameters are dimensionless and comparable in size. Mutual comparability of WA parameters is a desirable property. An inversion using WA parameters is naturally balanced and equally sensitive to all WA parameters (depending on data coverage only). Moveout formulae derived in this paper, for example, offer such an advantage. For another example, see the traveltime inversion by Růžek and Pšenčík (2014). In contrast, the complete set of Thomsen's parameters includes, in addition to non-dimensional anisotropy parameters, also velocities along the axis of symmetry. Due to significantly different magnitudes of the anisotropy parameters and the velocities, the inversion usually becomes unbalanced and heavily biased towards the velocities, making the recovery of the Thomsen anisotropy parameters difficult (especially when noisy data are used). Finally, it is interesting to point out that a similar advantage of WA parameterization holds with respect to the parameters $A_{\alpha\beta}$ in Voigt

notation, for which the diagonal parameters are larger than the off-diagonal ones.

All the above described differences of WA parameters from parameters introduced by Thomsen (1986) hold also for extensions of Thomsen's specification to lower-symmetry media.

The discussion above suggests that the WA parameterization could be a useful generalization for solving forward as well as inverse problems in arbitrary anisotropic media (i.e., of arbitrary anisotropy symmetry and strength), for both P- and S-waves. It may allow us to formulate universal solutions without a further need to modify our data-processing algorithms for each anisotropy symmetry separately.

The use of WA parameters in weakly anisotropic media has additional advantages. The use of weak-anisotropy approximation leads to complete separation of P-waves from S-waves, see, e.g. Farra and Pšenčík (2003), Pšenčík and Farra (2005). (In weakly anisotropic media of general anisotropy, quantities describing P wave propagation are specified by only 15 WA parameters, whereas S-wave quantities are described by all 21 WA parameters.) Thus there is no need for non-physical assumptions like the zero S-wave speed in some specific directions, see, e.g., Alkhalifah (2000a), used to suppress S-waves influence. Similarly, it may be also possible to derive alternative P-wave migration operators applicable to *generally anisotropic* media of moderate strength that are not affected by S-wave artifacts at all.

WA parameters can also be implemented outside the weak-anisotropy assumption. Due to their simple theoretical link to the density-normalized stiffness parameters $A_{\alpha\beta}$ on one hand, and their practical physical interpretation on the other (straightforward similarities to Thomsen parameters), WA parameters could be perhaps more natural choice even for some fundamental data-processing steps in anisotropic media of arbitrary symmetry and strength. For example, full waveform inversion (FWI) broadly used today could be designed in terms of WA parameters, which would be then directly used in the consequent anisotropic migration.

Various implementations of WA parameters is a subject of future research. In the following, we utilize WA parameters in the derivation of P-wave moveout approximation valid for up to monoclinic anisotropy symmetry.

Traveltime formula

Let us consider a Cartesian coordinate system whose x_3-axis is vertical and x_1- and x_2-axes are horizontal. Let us further consider a homogeneous layer, which may be transversely isotropic with horizontal or vertical axis of symmetry, orthorhombic or monoclinic. In all those cases, let us assume that the horizontal reflector underlying the mentioned layer is parallel to a plane of symmetry. Such an assumption is commonly used in the oil industry today, where symmetry axes/planes are often assumed to be perpendicular/parallel to the underlying bedding. In such cases, incident down-going and reflected up-going rays are situated in the vertical plane and are symmetric with respect to the normal to the reflector. As in Farra and Pšenčík (2013a), we start the derivations from the exact formula for the square of the traveltime T of an unconverted reflected P wave. The wave propagates from the source S to the reflector, hits it at the point O and then

propagates back to the receiver R. Points S and R are situated on a horizontal profile parallel to the x_1'-axis of a *local* Cartesian coordinate system whose origin coincides with the source S and also represents the origin of the *global* coordinate system x_i. Origin S and the vertical axes are common for both coordinate systems. The reflected ray is thus situated in vertical plane (x_1', x_3'), see Figure 1. The square of the exact traveltime of the reflected P wave has the form:

$$T^2(x) = \frac{4H^2 + x^2}{v^2(\mathbf{n})} \ . \tag{2}$$

Here x is the offset (distance between S and R) and H is the depth of the horizontal reflector (coinciding with the symmetry plane). $T = T(x)$ denotes the exact traveltime of the considered unconverted reflected P wave. Symbol $v = v(\mathbf{n})$ denotes the *ray velocity*, which is a function of the *phase vector* $\mathbf{n}$, i.e., the direction of the slowness vector $\mathbf{p} = \mathbf{n}/c$, where c denotes the *phase velocity*. The ray velocity $v(\mathbf{n})$ represents the size of the ray-velocity vector $\mathbf{v}(\mathbf{n})$ (also called group-velocity vector), $\mathbf{v}(\mathbf{n}) = v(\mathbf{n})\mathbf{N}$. Here $\mathbf{N}$ is a unit vector called *ray vector* specifying the ray direction. The ray velocity $v(\mathbf{n})$ is thus a velocity along the ray.

In the considered configuration, $v(\mathbf{n})$ is the same along the incident and reflected rays. This simplifies derivations considerably.

We can transform equation (2) using the notation commonly used in moveout analysis:

$$\bar{x} = \frac{x}{2H} \ , \qquad T_0 = \frac{2H}{\alpha_0} \ . \tag{3}$$

Here $\bar{x}$ is the normalized offset, α_0 is the vertical P-wave phase velocity, symbol T_0 denotes the two-way zero-offset traveltime. Using (3), equation (2) can be expressed as:

$$T^2(\bar{x}) = \alpha_0^2 T_0^2 \ \frac{1 + \bar{x}^2}{v^2(\mathbf{n})} \ . \tag{4}$$

Note that unlike the situation considered by Farra and Pšenčík (2013a,b), the phase vector $\mathbf{n}$ in equation (4) may deviate from the plane (x_1', x_3'), in which the ray is situated. In fact, the phase vector $\mathbf{n}$ may deviate considerably from the ray vector $\mathbf{N}$. The deviation is controlled by the difference between the phase and the ray velocities as can be clearly seen from the relation $\mathbf{n} \cdot \mathbf{N} = c/v$, which follows from a well-known identity $\mathbf{p} \cdot \mathbf{v} = 1$. (It follows from the eikonal equation $a_{ijkl} p_i p_l g_j g_k = 1$ and the expression $v_i = a_{ijkl} p_l g_j g_k$, where a_{ijkl} denotes an element of the density-normalized stiffness tensor and p_i and g_i are the components of slowness and polarization vectors $\mathbf{p}$ and $\mathbf{g}$.)

The ray vector $\mathbf{N}$, which is, in contrast to $\mathbf{n}$, situated in the plane (x_1', x_3'), can be easily determined from the configuration leading to equation (2), see Figure 1. Due to the symmetry of the studied problem, it does not matter if we consider the down-going (incident) or up-going (reflected) ray. If we take, for example, the incident ray, the vector $\mathbf{N}$, expressed in terms of the normalized offset $\bar{x}$, has the following components in the local coordinate system:

$$N_1' = \frac{\bar{x}}{\sqrt{1 + \bar{x}^2}} \ , \qquad N_2' = 0 \ , \qquad N_3' = \frac{1}{\sqrt{1 + \bar{x}^2}} \ . \tag{5}$$

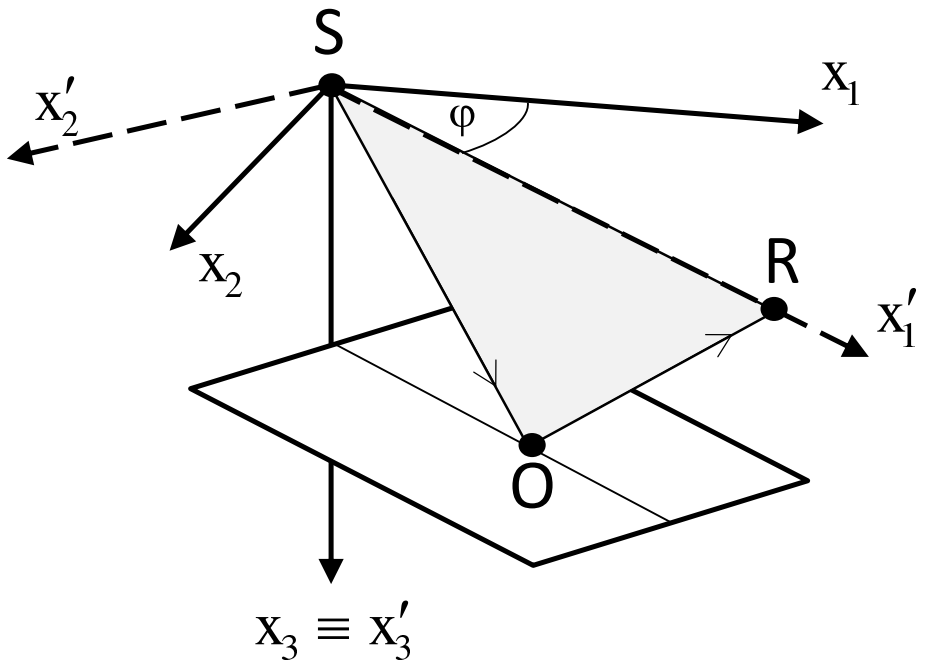

Figure 1: Schematic plot of the reflection experiment and of the two coordinate systems used: global coordinates x_i, local coordinates x_i'. φ - azimuth of the source receiver profile SR. SO - incident ray, OR - reflected ray.

For the evaluation of equation (4), we need to find v as a function of $\mathbf{n}$, which means that we need to find the direction of the slowness vector for a given ray direction $\mathbf{N}$. It is relatively simple to determine $\mathbf{N}$ from a given $\mathbf{n}$. However, to determine $\mathbf{n}$ corresponding to a given $\mathbf{N}$ is not such an easy task. For that we use approximate relations between $\mathbf{n}$ and $\mathbf{N}$ given by Farra and Pšenčík (2013a), resulting in an approximation for $v^2(\mathbf{n})$ to be used in equation (4).

Approximate ray-velocity expressions

Farra and Pšenčík (2013a) offer three following possibilities to approximately evaluate equation (4). In all of them, the first-order approximation $\tilde{c}^2(\mathbf{N})$ of the square of the phase velocity c is used.

1) *Ignore* the difference between the vectors $\mathbf{n}$ and $\mathbf{N}$ and express the square of the ray velocity v in terms of the *first-order approximation* of the square of the phase velocity c:
$$v^2(\mathbf{n}) = \tilde{c}^2(\mathbf{N}) \ . \tag{6}$$

2) *Take* the difference between the vectors $\mathbf{n}$ and $\mathbf{N}$ into account and express the square of ray velocity v in terms of the *first-order approximation* of the square of the phase velocity c:
$$v^2(\mathbf{n}) = \tilde{c}^2(\mathbf{N}) - \frac{4[B_{13}^2(\mathbf{N}) + B_{23}^2(\mathbf{N})]}{\tilde{c}^2(\mathbf{N})} \ . \tag{7}$$

3) *Take* the difference between vectors $\mathbf{n}$ and $\mathbf{N}$ into account and express the square of the ray velocity in terms of the *second-order* approximation of the square of the phase velocity c:
$$v^2(\mathbf{n}) = \tilde{c}^2(\mathbf{N}) + \frac{4a[B_{13}^2(\mathbf{N}) + B_{23}^2(\mathbf{N})]}{\tilde{c}^2(\mathbf{N})} \ . \tag{8}$$

In equation (8), $a = (r^2 - 3/4)/(1 - r^2)$, $r = \beta_0/\alpha_0$, where α_0 and β_0 are reference P- and S-wave velocities. We can chose them arbitrarily in principle. In order to simplify the following equations, we choose $\alpha_0^2 = A_{33}$ and $\beta_0^2 = A_{55}$, where $A_{\alpha\beta}$ are density-normalized elastic parameters in the Voigt notation. This choice implies $\epsilon_z = \gamma_y = 0$, see the WA parameters (1). Symbols B_{ij} in equations (7) and (8) denote elements of matrix $\mathbf{B}$, which plays an important role in the approximate expressions describing wave propagation in weakly anisotropic media. Matrix $\mathbf{B}$ is, in fact, Christoffel matrix rotated into a special coordinate system connected with the studied ray. More details and explicit expressions for the elements B_{13}, B_{23} and $\tilde{c}^2 = B_{33}$ in a monoclinic medium, whose plane of symmetry coincides with the plane (x_1, x_2) of the global Cartesian coordinate system x_i, are given in equations (A4) of Appendix A. In equations (B2) of Appendix B, elements $B_{13}(\mathbf{N})$, $B_{23}(\mathbf{N})$ and $B_{33}(\mathbf{N})$ are expressed in terms of the vector $\mathbf{N}$ situated in the plane (x_1', x_3') of the local coordinate system x_i' containing the source-receiver profile.

In the following, we use formulae (4) and (5) specified for the plane (x_1', x_3') containing the source-receiver profile. It means that in equations (6) - (8), we use B_{13}, B_{23} and $\tilde{c}^2 = B_{33}$ from equations (B2) expressed in terms of primed WA parameters (i.e., the parameters specified in the local coordinate system). We obtain moveout expressions

valid in the plane (x_1', x_3'). To obtain the moveout expressions in the global coordinate system for arbitrary orientation of the source-receiver profile, we can use equations (B3) providing the necessary transformation between the primed WA parameters and the WA parameters (1) specifying a monoclinic medium in global coordinates.

By inserting equations (5) into equations (B2) we obtain expressions for $B_{13}(\mathbf{N})$, $B_{23}(\mathbf{N})$ and $\tilde{c}^2(\mathbf{N}) = B_{33}(\mathbf{N})$ in terms of the normalized offset $\bar{x}$ and primed WA parameters:

$$B_{13}(\bar{x}) = \frac{\alpha_0^2 Q_1(\bar{x})}{2(1+\bar{x}^2)^2} \ , \quad B_{23}(\bar{x}) = \frac{\alpha_0^2 (1+\bar{x}^2)^{1/2} Q_2(\bar{x})}{2(1+\bar{x}^2)^2} \ , \quad \tilde{c}^2(\bar{x}) = \frac{\alpha_0^2 P(\bar{x})}{(1+\bar{x}^2)^2} \ . \tag{9}$$

Note that the third equation (9) represents the first-order approximation of the square of phase velocity c. In equations (9), symbols $P(\bar{x})$, $Q_1(\bar{x})$ and $Q_2(\bar{x})$ denote polynomials:

$$\begin{aligned} P(\bar{x}) &= (1+\bar{x}^2)^2 + 2\delta_y' \bar{x}^2 + 2\epsilon_x' \bar{x}^4 \ , \\ Q_1(\bar{x}) &= 2\bar{x}[2\epsilon_x' \bar{x}^2 + \delta_y'(1-\bar{x}^2)] \ , \\ Q_2(\bar{x}) &= 2\bar{x}(\chi_z' + \epsilon_{16}' \bar{x}^2) \ . \end{aligned} \tag{10}$$

Polynomial $P(\bar{x})$ contains terms of the zero and first order in the WA parameters, polynomials $Q_1(\bar{x})$ and $Q_2(\bar{x})$ contain only the first order terms.

Moveout formulae

We now have available all the necessary expressions needed for completing the derivations of the three moveout approximations in the plane (x_1', x_3').

Case 1

Equation (6) and the third equation of (9) yield:

$$v^2(\mathbf{n}) = \alpha_0^2 \frac{P(\bar{x})}{(1+\bar{x}^2)^2} \ . \tag{11}$$

Inserting equation (11) to (4), we obtain

$$T^2(\bar{x}) = T_0^2 \ \frac{(1+\bar{x}^2)^3}{P(\bar{x})} \ , \tag{12}$$

where $P(\bar{x})$ contains all the medium parameters and is given by equation (10). Using further the transformation relations (B3) inside $P(\bar{x})$, equation (12) becomes a 3D first-order traveltime formula for a monoclinic medium, which can be used for an arbitrary azimuth φ of the source-receiver profile. It was derived by ignoring the difference in the orientation of the vectors $\mathbf{n}$ and $\mathbf{N}$, and considering $v^2(\mathbf{n}) = \tilde{c}^2(\mathbf{N})$. Formulae for orthorhombic, HTI or VTI media can be obtained from (12) by specifying the two WA parameters ϵ_x' and δ_y', which appear in the polynomial $P(\bar{x})$ using expressions (B5), (B7) or (B9), respectively.

For zero offset, equation (12) yields correctly the square of the two-way zero-offset traveltime T_0. For long offsets, $\lim_{x\to\infty} T^2(x)/x^2$ yields $\tilde{c}_H^{-2}$, where $\tilde{c}_H^2 = \alpha_0^2(1+2\epsilon'_x)$ is the first-order approximation of the square of phase velocity in the horizontal direction, see the last equation in (B2).

In the source-receiver plane (x'_1, x'_3), the approximation (12) depends on four parameters: two-way zero-offset traveltime T_0 related to α_0, the depth H of the reflector and two primed WA parameters ϵ'_x and δ'_y. Parameter ϵ'_z is zero. Parameters ϵ'_x and δ'_y depend on 8 WA parameters using equations (B3) in monoclinic media, on 5 WA parameters using equations (B5) in orthorhombic media and on 2 WA parameters using equations (B7) and (B9) in HTI and VTI media, respectively. In all cases, $\epsilon_z = 0$. For VTI media, the obtained formulae are identical to formulae derived by Farra and Pšenčík (2013a).

By differentiating equation (12) with respect to the squared offset, we obtain corresponding expressions for the inverse of the square of the NMO velocity v_{NMO} and the quartic coefficient A_4 of the Taylor expansion of T^2 for a monoclinic medium:

$$v_{NMO}^{-2} = (1-2\delta'_y)/\alpha_0^2 \ . \tag{13}$$

$$A_4 = 2[\delta'_y - \epsilon'_x + 2(\delta'_y)^2]/\alpha_0^4 T_0^2 \ . \tag{14}$$

For more details, see Appendix C.

Case 2

Equation (7) and equations (9) yield

$$v^2(\mathbf{n}) = \alpha_0^2 \frac{P^2(\bar{x}) - Q_1^2(\bar{x}) - (1+\bar{x}^2)Q_2^2(\bar{x})}{P(\bar{x})(1+\bar{x}^2)^2} \ . \tag{15}$$

Inserting equation (15) to (4), we obtain

$$T^2(\bar{x}) = T_0^2 \ \frac{P(\bar{x})(1+\bar{x}^2)^3}{P^2(\bar{x}) - Q_1^2(\bar{x}) - (1+\bar{x}^2)Q_2^2(\bar{x})} \ . \tag{16}$$

Similarly to Case 1, WA parameters are contained inside the polynomials $P(\bar{x})$, $Q_1(\bar{x})$ and $Q_2(\bar{x})$ given by expressions (10). Inserting (B3) to (16), we obtain again a 3D first-order traveltime formula for a monoclinic medium, which can be used for an arbitrary azimuth φ. Unlike in equation (12), equation (16) takes into account the difference in orientation of vectors $\mathbf{n}$ and $\mathbf{N}$ and the square of the ray velocity is expressed in terms of the first-order approximation of the square of the phase velocity.

In the source-receiver plane (x'_1, x'_3), the approximation (16) depends on six parameters: two-way zero-offset traveltime T_0 related to α_0, the depth H of the reflector and four primed WA parameters ϵ'_x, δ'_y, χ'_z and ϵ'_{16}. Parameter ϵ'_z is again zero. As in Case 1, we can transform equation (16) to the form applicable to arbitrary orientation of the source-receiver profile and to any of considered anisotropy symmetries. Interestingly, the number of WA parameters, on which equation (16) depends in those cases, is the same as in the case of equation (12). Again, $\epsilon_z = 0$ in all cases. For VTI media, we obtain formulae identical to those derived by Farra and Pšenčík (2013a).

By differentiating equation (16) with respect to the squared offset, we obtain corresponding expressions for the inverse of the square of the NMO velocity v_{NMO} and the quartic coefficient A_4 of the Taylor expansion of T^2 for a monoclinic medium:

$$v_{NMO}^{-2} = [1 - 2\delta'_y + 4\Big((\delta'_y)^2 + (\chi'_z)^2\Big)]/\alpha_0^2 \ . \tag{17}$$

$$A_4 = \Big(2[\delta'_y - \epsilon'_x + 2(\delta'_y)^2] - 4[5(\delta'_y)^2 - 4\epsilon'_x\delta'_y + 2\chi'_z(\chi'_z - \epsilon'_{16})]\Big)/\alpha_0^4 T_0^2 \ . \tag{18}$$

For more details, see again Appendix C.

Case 3

Equation (8) and equations (9) yield

$$v^2(\mathbf{n}) = \alpha_0^2 \frac{P^2(\bar{x}) + a[Q_1^2(\bar{x}) + (1+\bar{x}^2)Q_2^2(\bar{x})]}{P(\bar{x})(1+\bar{x}^2)^2} \ . \tag{19}$$

Inserting equation (19) to (4), we obtain

$$T^2(\bar{x}) = T_0^2 \ \frac{P(\bar{x})(1+\bar{x}^2)^3}{P^2(\bar{x}) + a[Q_1^2(\bar{x}) + (1+\bar{x}^2)Q_2^2(\bar{x})]} \ . \tag{20}$$

Here again, $a = (r^2 - 3/4)/(1 - r^2)$ and $r = \beta_0/\alpha_0$. Polynomials $P(\bar{x})$, $Q_1(\bar{x})$ and $Q_2(\bar{x})$ are given in (10). Inserting (B3) to (20), we obtain a 3D second-order traveltime formula for a monoclinic medium, which can be used for an arbitrary azimuth φ. It can be, of course, reduced to any higher symmetry as orthorhombic, HTI or VTI. The formula takes into account the difference in the orientation of vectors $\mathbf{n}$ and $\mathbf{N}$, and the expression for the square of the ray velocity in terms of the second-order approximation of the square of the phase velocity.

In the source-receiver plane (x'_1, x'_3), the approximation (20) depends on seven parameters: two-way zero-offset traveltime T_0 related to α_0, the depth H of the reflector, four primed WA parameters ϵ'_x, δ'_y, χ'_z, ϵ'_{16} and parameter $r = \beta_0/\alpha_0$. Again, $\epsilon'_z = 0$. As in the VTI case studied by Farra and Pšenčík (2013a), the dependence on r is, however, weak. Therefore, if r is chosen close to the Poisson ratio, i.e., $r^2 \sim 1/3$ ($a \sim -5/8$), it is not necessary to consider it as a free parameter. The number of WA parameters, on which equation (20) depends in media of various anisotropic symmetries, is the same as in the case of equation (12). For VTI media, we, again, consistently obtain formulae as in Farra and Pšenčík (2013a).

By differentiating equation (20) with respect to the squared offset, we obtain corresponding expressions for the inverse of the square of the NMO velocity v_{NMO} and the quartic coefficient A_4 of the Taylor expansion of T^2 for a monoclinic medium:

$$v_{NMO}^{-2} = [1 - 2\delta'_y - 4a\Big((\delta'_y)^2 + (\chi'_z)^2\Big)]/\alpha_0^2 \ . \tag{21}$$

$$A_4 = \Big(2[\delta'_y - \epsilon'_x + 2(\delta'_y)^2] + 4a[5(\delta'_y)^2 - 4\epsilon'_x\delta'_y + 2\chi'_z(\chi'_z - \epsilon'_{16})]\Big)/\alpha_0^4 T_0^2 \ , \tag{22}$$

For details, see Appendix C.

Reference moveout formulae

To evaluate the accuracy of the above formulae for T^2, we compare T^2 obtained from them with that obtained from formula (3.37) of Tsvankin and Grechka (2011), derived for media of orthorhombic symmetry. In our notation, the formula (3.37) reads

$$T^2(\bar{x}) = T_0^2\Big(1 + A_2^T(\varphi)\bar{x}^2 + \frac{A_4^T(\varphi)\bar{x}^4}{1 + B(\varphi)\bar{x}^2}\Big) \ . \tag{23}$$

Here

$$A_2^T(\varphi) = \frac{\sin^2\varphi}{1+2\delta_1} + \frac{\cos^2\varphi}{1+2\delta_2} \ , \qquad A_4^T(\varphi) = -2\eta(\varphi)(A_2^T)^2(\varphi) \ ,$$
$$B(\varphi) = [1 + 2\eta(\varphi)]A_2^T(\varphi) \ , \qquad \eta(\varphi) = \eta_1 \sin^2\varphi - \eta_3 \sin^2\varphi\cos^2\varphi + \eta_2\cos^2\varphi \ , \tag{24}$$

where

$$\eta_1 = \frac{\epsilon_1 - \delta_1}{1+2\delta_1}, \qquad \eta_2 = \frac{\epsilon_2 - \delta_2}{1+2\delta_2}, \qquad \eta_3 = \frac{\epsilon_1 - \epsilon_2 - \delta_3(1+2\epsilon_2)}{(1+2\epsilon_2)(1+2\delta_3)} \ . \tag{25}$$

Parameters ϵ_1, ϵ_2, δ_1, δ_2 and δ_3 are parameters introduced by Tsvankin and Grechka (2011) as a generalization of Thomsen's (1986) parameters:

$$\epsilon_1 = \frac{A_{22} - A_{33}}{2A_{33}} \ , \qquad \epsilon_2 = \frac{A_{11} - A_{33}}{2A_{33}} \ , \qquad \delta_1 = \frac{(A_{23} + A_{44})^2 - (A_{33} - A_{44})^2}{2A_{33}(A_{33} - A_{44})} \ ,$$
$$\delta_2 = \frac{(A_{13} + A_{55})^2 - (A_{33} - A_{55})^2}{2A_{33}(A_{33} - A_{55})} \ , \qquad \delta_3 = \frac{(A_{12} + A_{66})^2 - (A_{11} - A_{66})^2}{2A_{11}(A_{11} - A_{66})} \ , \tag{26}$$

and φ is the azimuth measured from the (x_1, x_3) plane. Formula (23) is an extension of nonhyperbolic VTI moveout formula of Alkhalifah and Tsvankin (1995) to orthorhombic media, derived using the quasi-acoustic approximation (assuming $\beta_0 = 0$). In the symmetry planes ($\varphi = 0^o, 90^o$), equation (23) reduces to VTI moveout equation. For the off-symmetry directions, Tsvankin and Grechka (2011) use azimuthally varying NMO velocity $v_{NMO}(\varphi)$ (so-called NMO ellipse) and azimuthally varying parameter $\eta(\varphi)$ to derive equation (23). The parameter $\eta(\varphi)$ results from a simplification of complicated exact formula for the quartic coefficient of the traveltime expansion (Dajani et al., 1998) under the weak-anisotropy approximation. The accuracy of equation (23) for large offsets in off-symmetry directions is of the first-order. It is equivalent to the accuracy of our first-order formula (12), whose asymptote is $[\alpha_0^2(1 + 2\epsilon_x')]^{-1}$. The asymptote of formula (12) represents the inverse of the first-order approximation of the square of the phase velocity in the x_1' direction. Due to further improved accuracy, equations (16) and (20) give better accuracy for large offsets than equation (23). For example, second-order traveltime formula (20) has asymptote $[\alpha_0^2(1 + 2\epsilon_x' + 4a(\epsilon_{16}')^2/(1 + 2\epsilon_x')]^{-1}$. This asymptote represents the inverse of the second-order approximation of the square of the ray velocity in the x_1' direction. In the next section we illustrate this numerically on the model of an orthorhombic medium.

Tests of accuracy

Here we evaluate relative travel time errors $(T-T_{ex})/T_{ex}\times 100\%$ of formulae (12), (16) and (20), where T is the approximate traveltime calculated from the formulae to be tested and T_{ex} is the exact traveltime calculated using the package ANRAY, see Gajewski and Pšenčík (1990). We test the above formulae on models with varying anisotropy symmetry and strength. When appropriate, we compare the results of our formulae with results of reference formula (23). As a measure of P-wave anisotropy strength, we use the relation $2(V_{max}-V_{min})/(V_{max}+V_{min})\times 100\%$.

Three models consisting of two homogeneous horizontal layers separated by a horizontal reflector are considered. For each model, the reflector coincides with a plane of symmetry of the overlaying medium. The first, *HTI model*, with axis of symmetry parallel to the x_1-coordinate axis is derived from the Greenhorn shale model (Stovas, 2010), by making the vertical axis of symmetry horizontal. Farra and Pšenčík (2013a,b) used this model in their study of moveout in VTI media and in dip-constrained TI media (TI media whose axis of symmetry is perpendicular to a dipping reflector). P-wave anisotropy of this model is rather strong, about 26%. The second, orthorhombic *ORT model*, is the model used by Schoenberg and Helbig (1997). Its planes of symmetry coincide with coordinate planes and one of them is parallel to the reflector. P-wave anisotropy of this model is $\sim$ 25%. The third, monoclinic *MONO model*, is derived from the Vosges sandstone model of Mensch and Rasolofosaon (1997) by making the originally triclinic model monoclinic. Its single plane of symmetry coincides with the reflector. P-wave anisotropy is $\sim$ 15%. P-wave WA parameters for all three models are given in Table 1. Due to the choice $\alpha_0^2 = A_{33}$ (α_0 can be chosen arbitrarily, see the discussion of WA parameters above), WA parameter ϵ_z is zero in all models. Then, for the evaluation of moveout formulae in the HTI model we need 2, in the ORT model 5, and in the MONO model 8 WA parameters. Note that the number of required WA parameters is smaller than generally needed for the description of seismic attributes in the corresponding media. It is a direct consequence of using WA approximation, where P and S waves are fully separated (only P wave WA parameters are needed).

Model	α_0(km/s) r^2	β_0(km/s)	ϵ_x δ_x	ϵ_y δ_y	ϵ_{16} δ_z	ϵ_{26} χ_z
HTI	3.805 0.158	1.510	-0.169 –	– -0.373	– –	– –
ORT	2.437 0.337	1.414	0.258 0.077	0.328 -0.083	– 0.340	– –
MONO	2.604 0.362	1.566	-0.135 -0.128	-0.124 -0.057	0.057 -0.241	-0.043 -0.071

Table 1: Parameters of the models used in tests. α_0 and β_0: P- and S-wave reference velocities; $r^2=\beta_0^2/\alpha_0^2$; ϵ_x, ϵ_y, ϵ_{16}, ϵ_{26}, δ_x, δ_y, δ_z and χ_z: P-wave WA parameters; $\epsilon_z=0$.

Figure 2 shows the relative P-wave traveltime errors versus the normalized offset $\bar{x} = x/2H$ for the HTI model. Similarly as the traveltimes themselves, the errors vary with azimuth φ. Since the variations are quite pronounced, we show the traveltime error curves for a dense system of azimuths (color-coded). In the left column, traveltime errors for azimuths $\varphi = 0^o$, 30^o, 45^o, 50^o, and in the right column for $\varphi = 60^o$, 70^o, 80^o and 90^o are shown. The azimuths are measured from the x_1-axis, which is parallel to the symmetry axis. The plots on the top correspond to the first-order equation (12) ignoring different directions of the ray and phase vectors $\mathbf{N}$ and $\mathbf{n}$, respectively. The plots in the middle correspond to the first-order equation (16), taking into account the different directions of $\mathbf{N}$ and $\mathbf{n}$. The bottom row shows the errors using the second-order equation (20). As expected, we can observe increasing accuracy from the top to the bottom. While maximum errors of equation (12) are around 2.5%, they are less than 2% for equation (16), and around 0.7% for equation (20).

Best results with all formulae are obtained, of course, in the isotropy plane, perpendicular to the axis of symmetry, i.e., for $\varphi = 90^o$. This is obvious because squares of all the ray-velocity approximations yield α_0^2, i.e., the exact value. Except for the interval of $\bar{x} \sim 0 - 2$, very good results are also obtained along the profile $\varphi = 0^o$. With increasing deviations of profiles from $\varphi = 0^o$, larger errors extend to larger offsets. For $\varphi \sim 45 - 60^o$, the errors reach their maximum, for larger azimuths, they successively decrease to zero for $\varphi = 90^o$. As in the VTI case (Farra and Pšenčík, 2013a), this behavior is directly related to the deviations of phase and ray vectors $\mathbf{n}$ and $\mathbf{N}$ as shown in Figure 3.

In Figure 3, the top row contains plots of the exact phase and ray velocities as functions of the normalized offset $\bar{x}$ along selected profiles. For each profile specified by a different color, we show two curves. The upper curve (full) corresponds to the ray (group) velocity, the lower one (dashed) to the phase velocity. For all azimuths, except $\varphi = 90^o$, which corresponds to the isotropy plane, we observe rather sharp decrease of both velocities at small offsets. At offsets greater than $\bar{x} \sim 2$, the velocities are nearly constant. The rate of change at small offsets decreases with increasing azimuth φ. For a given azimuth, the differences in between the phase c and ray v velocities are directly correlated with differences in between the phase and ray vectors $\mathbf{n}$ and $\mathbf{N}$, respectively, shown in the middle row of Figure 3. Specifically, the deviation of the two vectors $\mathbf{n}$ and $\mathbf{N}$ is controlled by the relation $\mathbf{N} \cdot \mathbf{n} = c/v$ (all quantities involved being taken for the same phase direction). We can see that, as in the VTI case studied by Farra and Pšenčík (2013a), the maximum deviations can reach non-negligible 16^o. Similarly to the velocities, the difference in between the vectors $\mathbf{n}$ and $\mathbf{N}$ quickly varies for small offsets (fastest being the azimuth of the symmetry axis, $\varphi = 0^o$), and becomes nearly constant at large offsets.

The bottom plot in Figure 3 shows variation of NMO velocity v_{NMO} with azimuth, for $\varphi = 0^o - 180^o$. The results of the first-order formula (13), see also (C13) with (C18), in which the different directions of $\mathbf{N}$ and $\mathbf{n}$ are ignored, are shown in blue, the results of the second-order formula (21), see also (C13) with (C19), are in red. The exact NMO velocity is shown in black for comparison. All three NMO velocities coincide for the azimuth of 90^o (isotropy plane), maximum differences being along the axis of symmetry. The accuracy of the above proposed weak-anisotropy formulae depends, of course, on the strength of anisotropy. Anisotropy of the HTI model is $\sim 26\%$, which cannot be considered weak. The accuracy is also affected by the magnitude of δ_y. Specifically, it can be seen from equations (C18) and (C19) that the values of the approximate v_{NMO}

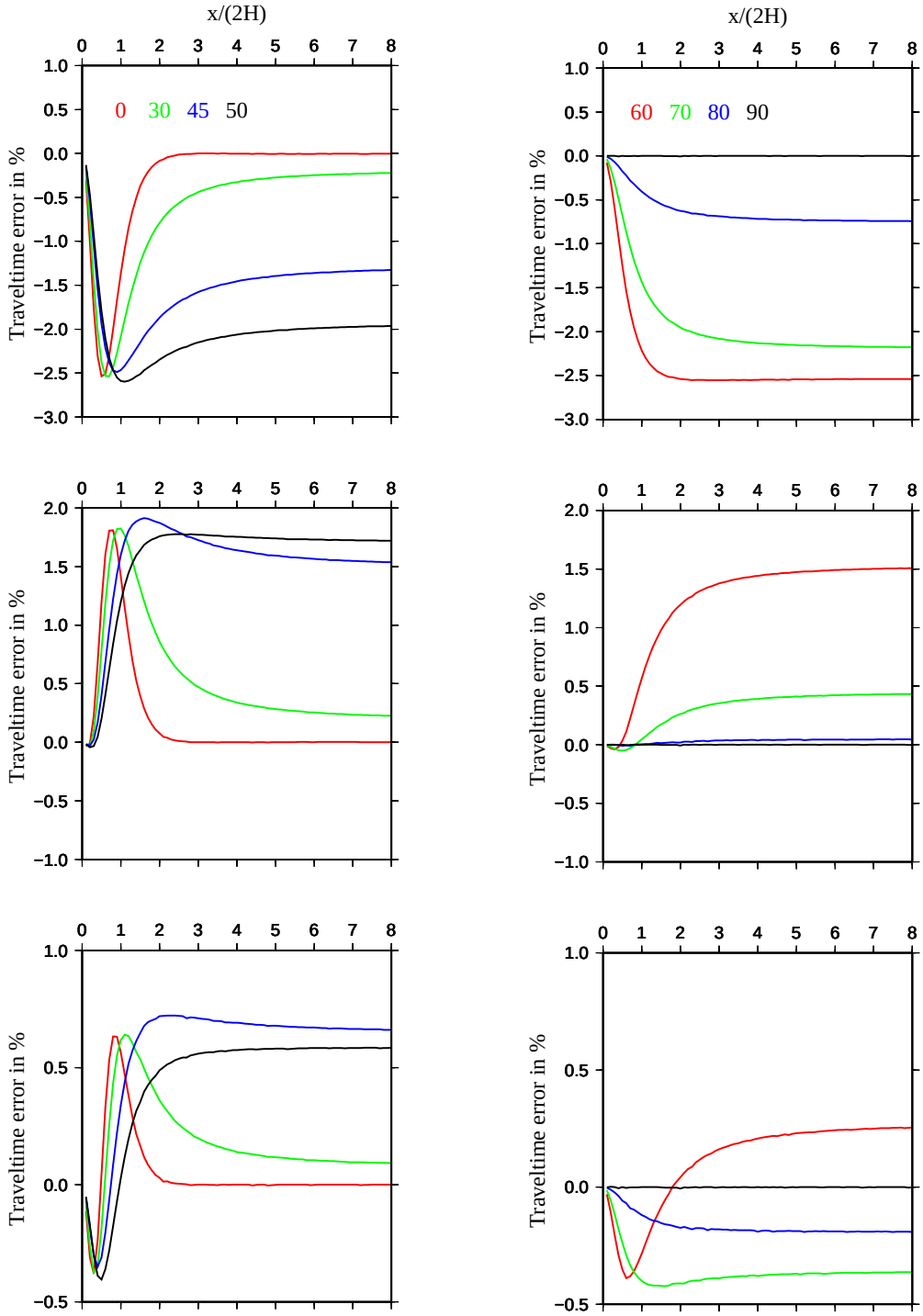

Figure 2: HTI model; anisotropy $\sim 26\%$. Variation of relative traveltime errors with the normalized offset $\bar{x} = x/2H$, calculated with the first-order approximation (12) ignoring different directions of $\mathbf{N}$ and $\mathbf{n}$ (top), with the first-order approximation (16) taking into account different directions of $\mathbf{N}$ and $\mathbf{n}$ (middle) and with the second-order approximation (20) (bottom). Relative errors are estimated along profiles with azimuth $\varphi = 0^o$, 30^o, 45^o, 50^o (left), 60^o, 70^o, 80^o and 90^o (right), measured from the x_1-axis (parallel with the symmetry axis).

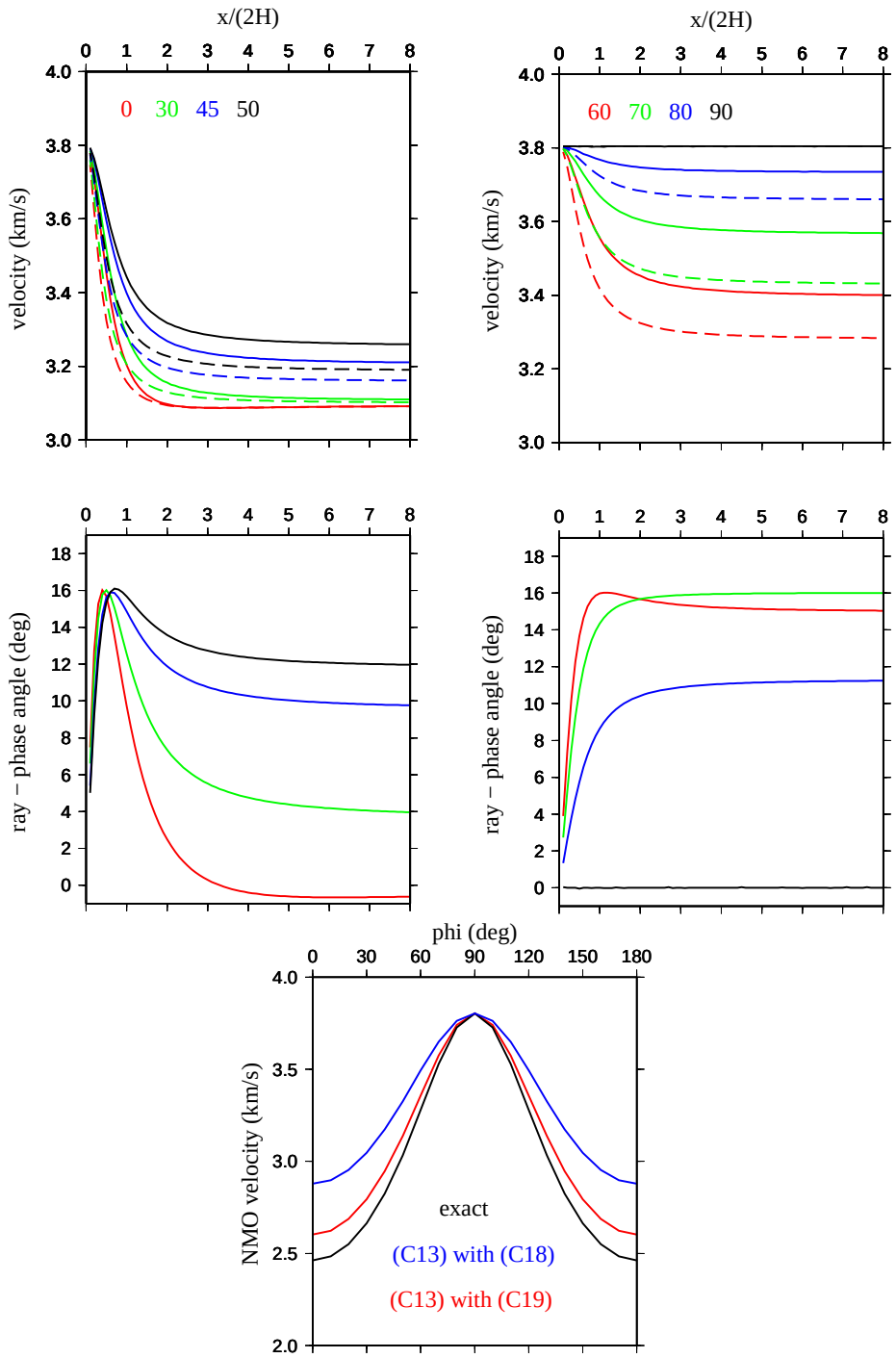

Figure 3: HTI model; anisotropy $\sim$ 26%. Top: variation with the normalized offset $\bar{x} = x/2H$ of exact phase and ray velocities for azimuths $\varphi = 0^o$, 30^o, 45^o, 50^o (left) and 60^o, 70^o, 80^o and 90^o (right), measured from the x_1-axis (parallel with the symmetry axis). The phase (dashed) and ray (full) velocity for each φ are plotted by the same color. Middle: variation of angular differences of exact ray- and phase-velocity directions **N** and **n** for the same azimuths as above. Bottom: variation of NMO velocity with azimuth φ. Comparison of the first-order formula (C13) and (C18), ignoring different directions of **N** and **n** (blue), and the second-order formula (C13) and (C19) (red) with the exact formula (black).

vary around the background P-wave velocity α_0, which was chosen as the vertical velocity. The variations for the maximum-error azimuths $\varphi = 0^o$ and 180^o are controlled by the parameter δ_y, which is, in this case, quite large, see Table 1. The exact NMO velocity for these azimuths is 2.46 km/s while eq.(13) yields 2.88 km/s (blue) and eq.(21) 2.6 km/s (red). On the other hand, for the azimuth $\varphi = 90^o$, for which the approximate v_{NMO} is independent of WA parameters, it coincides with the exact v_{NMO} (3.805 km/s) and with $\alpha_0 = \sqrt{A_{33}}$.

Figure 4 summarizes the results for the ORT model. In the left column, we can see the relative P-wave traveltime errors versus the normalized offset $\bar{x}$ obtained from formulae (12) at the top, (16) in the middle and (20) at the bottom (analogy to Figure 2 for HTI medium). Although the traveltime error distribution is somewhat different from that in Figure 2, the overall accuracy of the approximations (12), (16) and (20) for ORT medium ($\sim 25\%$ anisotropy) is fairly comparable to that of the HTI, $\sim 26\%$ anisotropy. (Maximum errors obtained for ORT medium with equation (12) are approximately 2.8%, 2% for equation (16), and do not exceed 0.6% for equation (20)). This observation holds despite the different anisotropy symmetries and different characters of the ORT and HTI velocities: unlike in the HTI case, ORT velocity slowly increases with increasing offset and varies only moderately with azimuth (compare the top-right plot of Figure 3 with the top-right plot of Figure 4). Again, we can observe a clear correlation in between the large differences of the phase and ray velocities (top-right, Figure 4) and the large deviations of vectors $\mathbf{N}$ and $\mathbf{n}$ (middle-right, Figure 4). Maximum deviation of the vectors $\mathbf{N}$ and $\mathbf{n}$ is even slightly larger than in the HTI case, approximately 17^o. For azimuth $\varphi = 0^o$ (red), we can observe a change of mutual positions of vectors $\mathbf{n}$ and $\mathbf{N}$ at about $\bar{x} = 0.3$ (the angle between $\mathbf{n}$ and $\mathbf{N}$ changes from negative to positive).

The bottom-right plot in Figure 4 shows the variation of NMO velocity with azimuth, for $\varphi = 0^o - 180^o$. As in Figure 3, the results of the first-order formula (13), see also (C13) with (C16), are in blue, the results of the second-order formula (21), see (C13) with (C17), are in red. The exact NMO velocity is in black (it was obtained by using exact coefficients of Grechka et al. (2000) in (C13)). Interestingly, although anisotropy of the ORT model is also rather strong, about 25%, (compared to 26% of HTI), both v_{NMO} approximations work better here than in the HTI case. Moreover, in the case of the second-order formula (21), the approximate and exact curves nearly coincide. The reason is that the values of δ_x and δ_y are considerably smaller compared to the corresponding δ_y in the HTI case, see Table 1. The exact NMO velocities for azimuths $\varphi = 0^o$ and 90^o are 2.239 and 2.629 km/s, respectively. Corresponding values obtained with formula (13) are 2.258 and 2.651 km/s, and 2.242 and 2.628 km/s with formula (21), respectively.

In Figure 5, the relative P-wave traveltime errors of approximate formulae (12), (16) and (20) are compared with the errors obtained using the reference formula (23) by Tsvankin and Grechka (2011). The comparison is shown for four azimuths, 0^o, 30^o, 60^o and 90^o. The red curves represent the relative P-wave traveltime errors of the first-order formula (12), the green curves of the first-order formula (16) and the blue curves represent the second-order formula (20). The curves corresponding to the reference formula (23) are black. The accuracy of the first-order approximations (formulae (12) and (16)) is generally comparable with that of Tsvankin and Grechka (2011), with the relative errors within $\pm 2.5\%$ range. The second-order approximation (20) seems to perform consistently better, with an error not exceeding $\pm 0.5\%$. Relative errors of formulae (12), (16) and

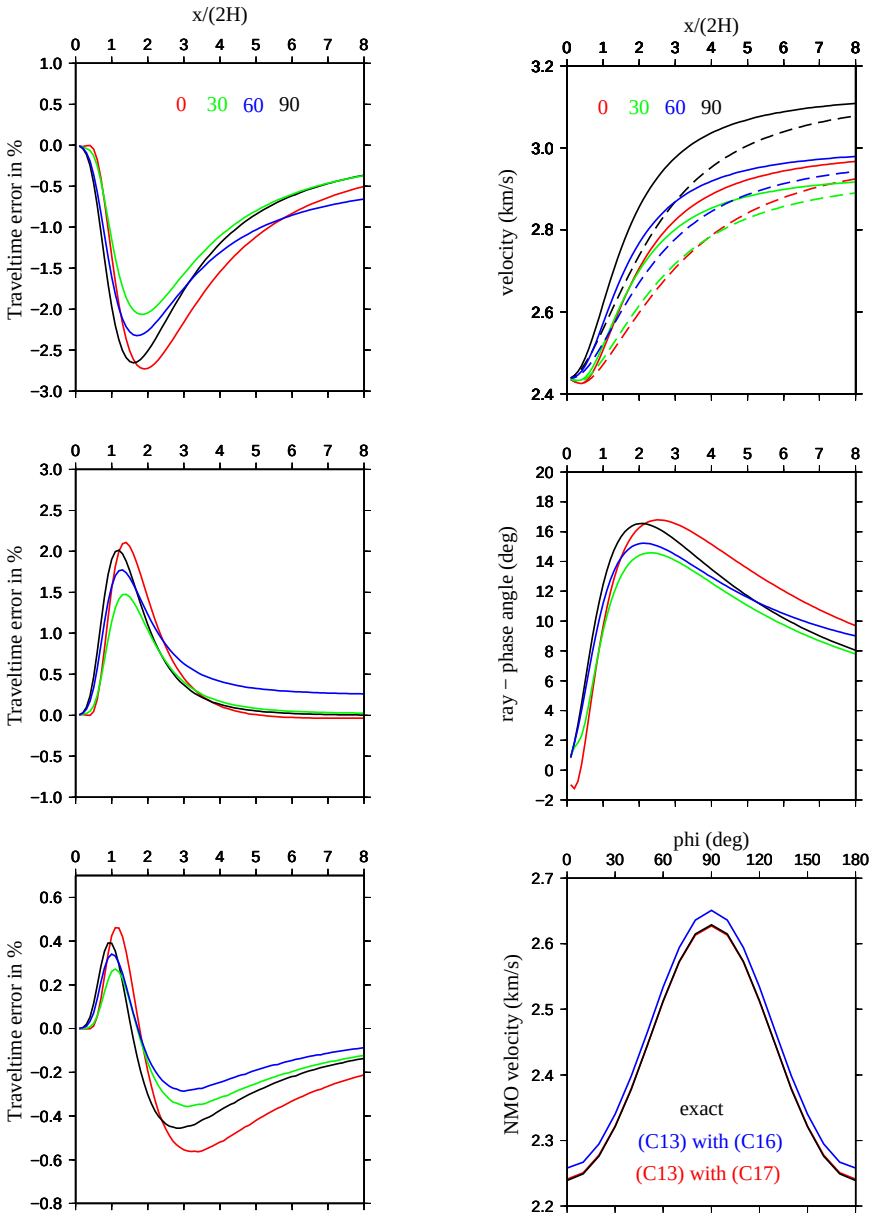

Figure 4: ORT model; anisotropy $\sim 25\%$. Left column: variation with the normalized offset $\bar{x} = x/2H$ of relative traveltime errors calculated with the first-order approximation (12) ignoring different directions of $\mathbf{N}$ and $\mathbf{n}$ (top), with the first-order approximation (16) taking into account different directions of $\mathbf{N}$ and $\mathbf{n}$ (middle) and with the second-order approximation (20) (bottom). Relative errors are estimated along profiles with azimuths $\varphi = 0^o$, 30^o, 60^o and 90^o, measured from the x_1-axis. Right column: Top: variation of exact phase and ray velocities with $\bar{x}$ for azimuths $\varphi = 0^o$, 30^o, 60^o and 90^o, measured from the x_1-axis. The phase (dashed) and ray (full) velocities for each φ are plotted by the same color. Middle: variation of angular differences of exact ray and phase vectors $\mathbf{N}$ and $\mathbf{n}$ for the same azimuths as above. Bottom: variation of NMO velocity with azimuth φ. Comparison of the first-order formula (C13) and (C16) ignoring different directions of $\mathbf{N}$ and $\mathbf{n}$ (blue) and the second-order formula (C13) and (C17) (red) with the exact formula (black).

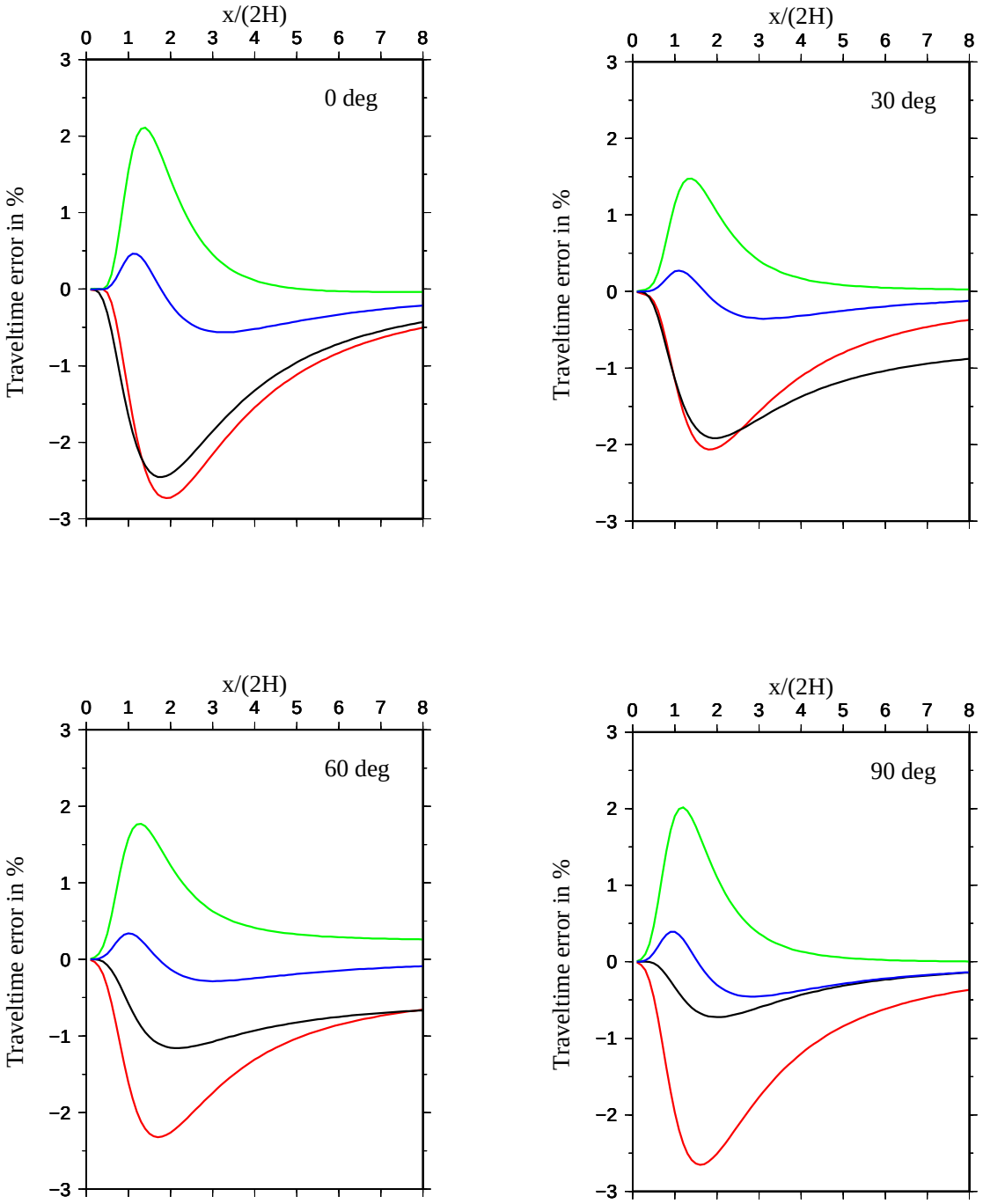

Figure 5: ORT model; anisotropy $\sim 25\%$. Comparison of accuracy: relative traveltime errors calculated for azimuths $\varphi = 0^o$, 30^o, 60^o and 90^o, using the first-order approximation (12) ignoring difference in directions of vectors $\mathbf{N}$ and $\mathbf{n}$ (red), the first-order approximation (16) taking into account different directions of $\mathbf{N}$ and $\mathbf{n}$ (green), and the second-order approximation (20) (blue) in comparison with Tsvankin and Grechka (2011) equation (23) (black).

(20) can be explained by the differences in between the phase and ray vectors **n** and **N**, respectively, as they vary with offset and azimuth - the error increases with increasing deviation of **N** from **n** and vice versa (see Figure 4). On the other hand, a physical explanation of relative errors of the reference formula (23) is not straightforward - the approximation (23) represents a formal expansion of T^2, which allows no physical insight.

Lastly, in analogy to Figures 2, 3 and 4, Figures 6 and 7 show the results for the MONO model. In Figure 6, as in the case of HTI model, the curves of the relative errors versus normalized offset vary quite significantly with azimuth (note that the variations are not symmetric around the azimuth $\varphi = 90^o$ in this case). The errors are, however, considerably smaller than those in the HTI case (anisotropy of MONO model is "only" about 15%). They reach their maximum of about 1.6% around the azimuth of $\phi = 150^o$ for the first-order approximations (12) and (16), mostly being smaller than 1%. The second-order approximation (20) is considerably more accurate, with its maximum error of about 0.4% (and less than 0.15% for most offsets and azimuths).

A good performance of the derived approximations in Figure 6 depends mostly on the anisotropy strength, rather than anisotropy symmetry, as demonstrated in Figure 7. Variation of the ray and phase velocities with the normalized offset shown at the top of Figure 7 is similar to that of the HTI model for azimuths from 0^o to 50^o, but differs beyond 50^o. The drop of velocities is more moderate, and the variation of the corresponding deviations of vectors **n** and **N** with $\bar{x}$ (middle row of Figure 7) has an opposite trend (maximum deviation is only about 14^o). Note that anisotropy of MONO model is about 15% compared to 26% of the HTI model.

The bottom plot in Figure 7 shows again variation of NMO velocity with azimuth, for $\varphi = 0^o - 180^o$. First-order formula (13), see also (C13) with (C14), shown in blue, yields highly accurate results around $\varphi = 150^o$. Largest deviations can be observed for $\varphi = 60^o$, but they are considerably smaller than the deviations in Figure 3. Second-order formula (21), see also (C13) with (C15), shown in red, yields results nearly identical with the exact v_{NMO} (black). The results for the MONO model suggest that the accuracy of the derived approximations is not compromised by lower anisotropy symmetry.

Conclusions

We discussed weak anisotropy (WA) parameterization suitable for forward and inverse seismic problems in models of arbitrary anisotropic symmetry and strength. The name weak anisotropy is, in this respect, misleading. The 21 WA parameters represent a fully equivalent alternative to the set of 21 elastic parameters $C_{\alpha\beta}$ or their density-normalized counterparts $A_{\alpha\beta}$. Due to their mutual linear relationships, one set can be easily converted to another and vice versa. Consequently, every theoretical development using $A_{\alpha\beta}$ can be easily re-parameterized in terms of WA parameters as well. In contrast to $A_{\alpha\beta}$, however, WA parameters have clear physical interpretation and relation to measurable data similarly to Thomsen-type parameterization (Thomsen, 1986). WA parameters constitute measurable *combinations* of $A_{\alpha\beta}$. This becomes a clear advantage in inversion problems. Additionally, and unlike Thomsen-type parameters, all WA parameters are unitless and of the same order of magnitude. Resulting inversion is thus well-balanced in terms of its sensitivity to individual WA parameters (therefore no need for any mutual parameter weighting and unit matching inside the inversion scheme).

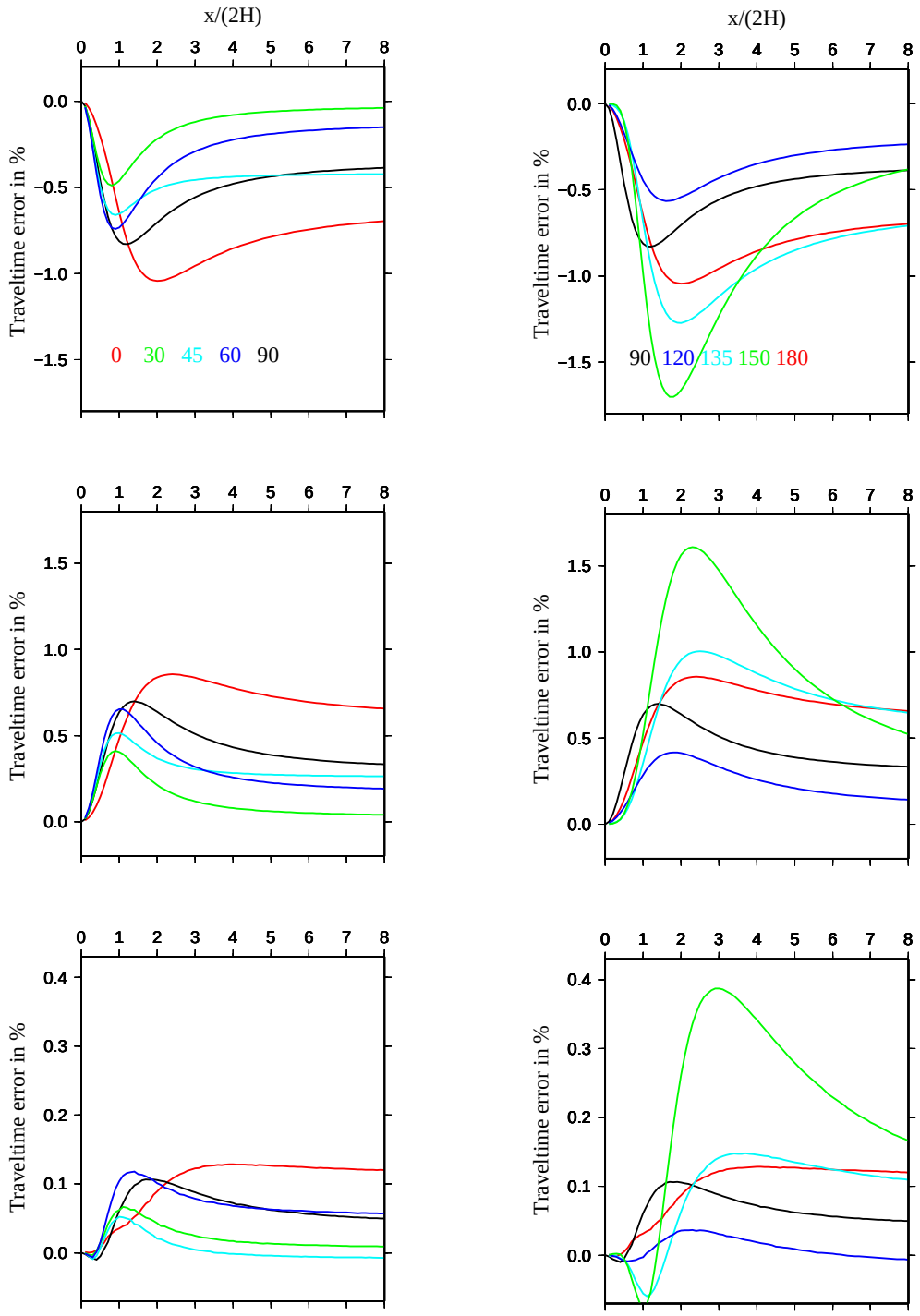

Figure 6: MONO model; anisotropy $\sim 15\%$. Variation with the normalized offset $\bar{x} = x/2H$ of relative traveltime errors, calculated with the first-order approximation (12) ignoring different directions of $\mathbf{N}$ and $\mathbf{n}$ (top), with the first-order approximation (16) taking into account different directions of $\mathbf{N}$ and $\mathbf{n}$ (middle) and with the second-order approximation (20) (bottom). Relative errors are estimated along profiles with azimuth $\varphi = 0^o$, 30^o, 45^o, 60^o, 90^o (left), 90^o, 120^o, 135^o, 150^o and 180^o (right), measured from the x_1-axis.

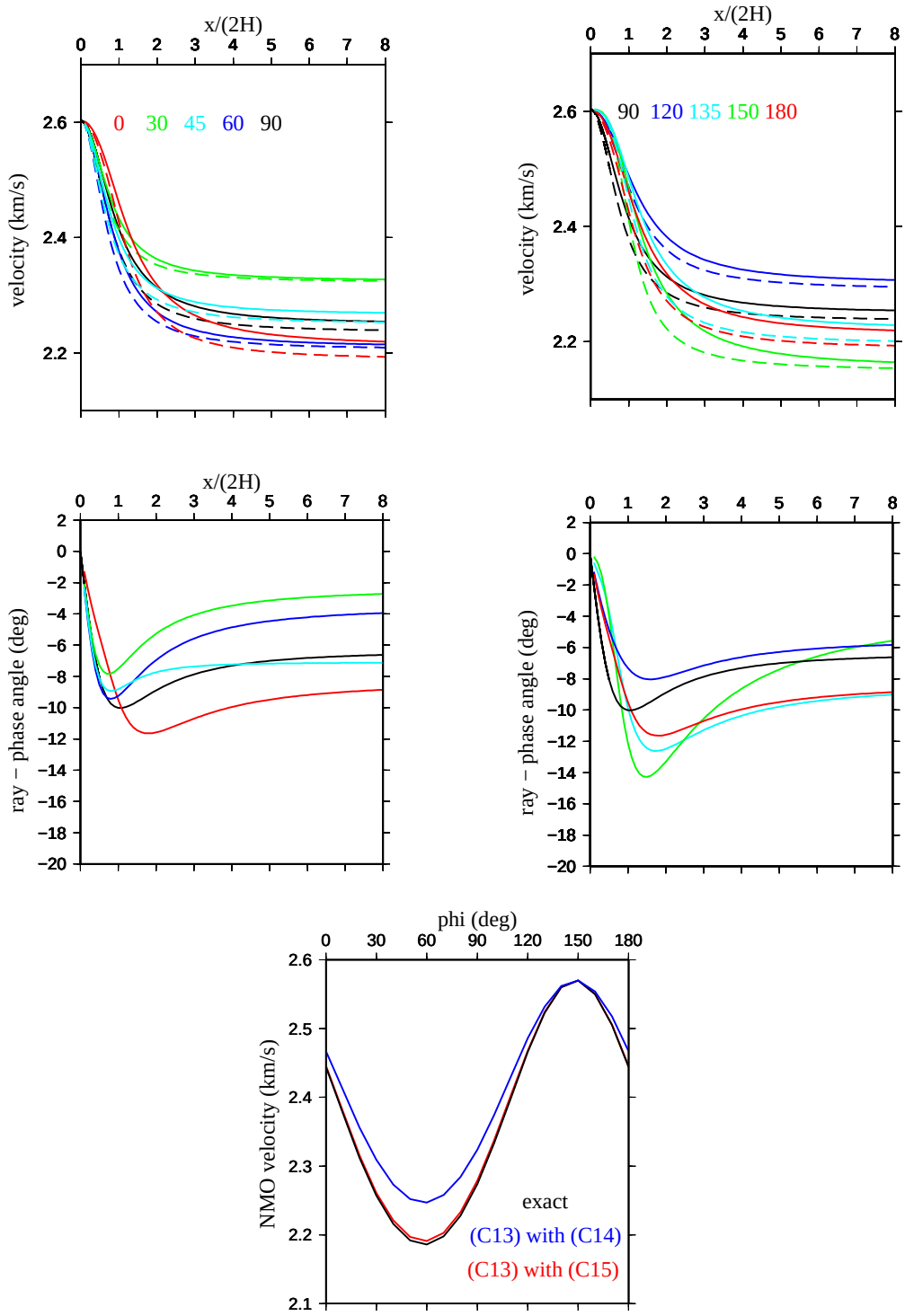

Figure 7: MONO model; anisotropy $\sim 15\%$. Top: Variation with the normalized offset $\bar{x} = x/2H$ of the exact phase and ray velocities for azimuths $\varphi = 0^o$, 30^o, 45^o, 60^o, 90^o (left) and 90^o, 120^o, 135^o, 150^o and 180^o (right), measured from the x_1-axis. The phase (dashed) and ray (full) velocities for each φ are plotted by the same color. Middle: variation of angular differences of the exact ray and phase vectors $\mathbf{N}$ and $\mathbf{n}$ for the same azimuths as above. Bottom: variation of NMO velocity with azimuth φ. Comparison of the first-order formula (C13) and (C14) ignoring different directions of $\mathbf{N}$ and $\mathbf{n}$ (blue) and second-order formula (C13) and (C15) (red) with the exact formula (black).

For these attractive properties, WA parameterization can offer a universal parameterization in seismic processing today when various anisotropy symmetries are proposed and tested. There is no need to re-design processing algorithms, including FWI or migrations, with each anisotropy symmetry once WA parameterization is adopted.

Apart from providing useful physical insights, WA parameterization offers an additional advantage when applied in *weakly-anisotropic settings* (hence their name): it allows full separation of P- from S-waves (for example, WA migration operators would not suffer from S-wave artifacts, no need for often-used zero S-wave velocity assumption, etc.). The consequence of the latter property is that the resulting accuracy of weak-anisotropy approximations can often be good enough, from practical standpoint, without a further need for more complex exact expressions. The accuracy can be further easily improved by adding higher order terms, as demonstrated in this paper on the example of traveltime approximations.

WA parameters are then used in the derivation of weak-anisotropy approximation moveout formulae for unconverted reflected P waves for transversely isotropic media with horizontal or vertical axis of symmetry, and for orthorhombic and monoclinic media. In all cases, the horizontal reflector coincides with a symmetry plane of the considered medium. This weak-anisotropy approach fundamentally differs from the well-known published derivations using Taylor expansions of T^2 with respect to the square of the offset. Several alternative WA traveltime formulae are presented here of different degrees of complexity and accuracy. In addition to traveltime, we also present corresponding approximations for the NMO velocities and the quartic term of the nonhyperbolic expansion.

Let us point out several attributes of herein derived approximations.

1) The WA formulae derived here are based on the weak-anisotropy approximation, which is the only assumption. No Taylor expansions of traveltime are used. This guarantees good behavior at all offsets as long as the weak-anisotropy assumption holds. Accuracy at large offsets may be important especially today when (extra) large-offset acquisitions become more frequent.

2) Despite the assumption of weak anisotropy, the numerical tests suggest that the weak-anisotropy approximations can work well even for 20% anisotropy, which may be sufficient for practical applications.

3) Non-physical assumptions as used, for example, in the so-called acoustic approximation (Alkhalifah, 2000a), are not necessary to obtain relatively simple and accurate WA approximations.

4) Unlike in Taylor expansions of traveltimes, our weak-anisotropy formulae need no additional corrections at large offsets, see, e.g. Tsvankin and Thomsen (1994). For VTI, the formulae even yield exact long-offset asymptote. For other types of anisotropy, the long-offset asymptotes are generally only approximate, which is the consequence of the weak-anisotropy assumption.

5) With the choice of the vertical P-wave velocity $\alpha_0^2 = A_{33}$ in WA parameterization, which leads to elimination of one of the WA parameters ($\epsilon_z = 0$), one needs 2, 5 or 8

WA parameters to describe P-wave moveout in a transversely isotropic, orthorhombic or monoclinic medium, respectively. This reduces the number of parameters otherwise needed for the moveout description in such media (5, 9 or 12 parameters, respectively).

6) As shown by Farra and Pšenčík (2013a) and as confirmed in this paper, our formulae yield results of a comparable, but often better accuracy than, for example, long-spread moveout formula of Alkhalifah and Tsvankin (1995), see also Alkhalifah (2000b) or Tsvankin (2001).

7) Because of their simple structure (no square roots, for example), our formulae are well suited for inversion of observed traveltimes for WA parameters utilizing fairly simple inversion schemes. For example, in the case of the traveltime approximation (12), which is the simplest approximation presented here, the problem reduces to an inversion of a system of linear equations.

8) When inverted, WA parameters can be immediately used for the description of other wave attributes (velocities, polarization, etc., see, e.g., Farra and Pšenčík, 2003).

9) Because of their linear relation to the elastic parameters $C_{\alpha\beta}$ (in Voigt notation), WA parameters and the quantities they parameterize transform in a simple fashion with a rotation of the coordinate system. This convenient property is utilized in the presented work to extend the expressions originally derived for a single source-receiver profile to all azimuths. This property can also be very useful in practical inversion problems while handling 2D/3D rotated anisotropic symmetries (TI or orthorhombic dipping layers, for example), when the relation between WA parameters in the local and global coordinate systems is straightforward. Such a simple transformation is, for example, impossible to do with δ parameter of Thomsen (1986), Tsvankin (1997) or Grechka et al. (2000).

10) The transformation property is also used in the derivation of azimuthally dependent quartic coefficient of the Taylor expansion of T^2 for orthorhombic and monoclinic media. In comparison with analogous approximation (3.37) of Tsvankin and Grechka (2011), no acoustic approximation was used (Dajani et al., 1998; Tsvankin and Grechka, 2011), and the accuracy of the resulting quartic coefficient was either comparable or higher than that given by Tsvankin and Grechka (2011).

11) Most of the presented formulae represent first-order weak-anisotropy approximation. It is straightforward to enhance the accuracy of these formulae by developing second-order approximations. Of course, this leads to slightly more complicated formulae containing squares of WA parameters, but no square roots. Importantly, the same set of WA parameters is required for both the first- or second-order approximations.

12) An important byproduct of the derivations here is a set of approximations for the ray velocity. Our first-order approximations might not be as accurate as, for example, Fomel's (2004), but they have certainly much simpler form (no square roots, for example, opposite to Fomel's VTI formula (29)). Moreover, our formulae hold for a general anisotropy. Another advantage of our formulae is that they provide an analytical relation between the ray (group) velocity and the ray angle, which, for example, Alkhalifah (2000b) was seeking.

13) As shown by Farra and and Pšenčík (2013b), the moveout formulae can be generalized for dip-constrained transversely isotropic (DTI) media (media with axis of symmetry perpendicular to a generally dipping reflector).

14) Generalization to layered media can be done using effective medium parameters, following the approach of Tsvankin (2001), Ursin and Stovas (2006), Tsvankin and Grechka (2011).

15) Presented formulae can be simply generalized for coupled shear waves, see Bakker (2002), Klimeš, (2006) Farra and Pšenčík (2008, 2010).

The proposed approximations were tested on models of varying anisotropy symmetry and anisotropy strength. The tests suggest that the accuracy of the formulae does not depend on the anisotropy symmetry. It is controlled by the anisotropy strength. The distribution of the errors with offset and azimuth of the presented approximations clearly correlates with the deviation of phase- and ray-velocity directions (caused by differences between the phase and ray velocities). This phenomenon has already been observed in previous studies (Farra and Pšenčík, 2013a, b). Despite the weak-anisotropy assumption, the tests suggest that especially the second-order traveltime formula yields results with a high accuracy: the maximum relative traveltime errors are well below 1% for anisotropy around 25%.

Finally, the presented formulae were derived with a practical use on mind, considering the increasing need for including lower anisotropy symmetries in seismic data processing today, and keeping the processing steps reasonably simple, adaptable and transparent at the same time. The presented formulae are, of course, only approximations, but their accuracy, which could be controlled to some degree, may become acceptable in many practical settings. It is only a first step but approximations like those derived here, complemented by a suitable medium parameterization such as WA parameterization, could provide a framework for seismic data processing in generally anisotropic media in future.

Acknowledgement

A substantial part of this work was done during IP's stay at the IPG Paris at the invitation of the IPGP. We are grateful to project "Seismic waves in complex 3-D structures" (SW3D) and Research Project 210/11/0117 of the Grant Agency of the Czech Republic for support. We thank BP America for support of SW3D project.

Appendix A

Matrix **B** *and WA parameters in global Cartesian coordinates*

Let us consider a global Cartesian coordinate system with the x_3-axis vertical, positive downwards. The elements B_{mn} of matrix **B** used in the approximate expressions in the text are given by the formula

$$B_{mn}(\mathbf{n}) = a_{ijkl} n_j n_l e_i^{[m]} e_k^{[n]}. \qquad (A1)$$

Here a_{ijkl} are density-normalized elastic moduli (elements of the stiffness tensor). Symbols n_i denote components of a unit vector **n**. Unit, mutually perpendicular vectors $\mathbf{e}^{[i]}$ are defined in the following way:

$$\mathbf{e}^{[1]} \equiv D^{-1}(n_1 n_3, n_2 n_3, n_3^2 - 1), \quad \mathbf{e}^{[2]} \equiv D^{-1}(-n_2, n_1, 0), \quad \mathbf{e}^{[3]} = \mathbf{n} \equiv (n_1, n_2, n_3), \quad (A2)$$

where

$$D = (n_1^2 + n_2^2)^{1/2}, \quad n_1^2 + n_2^2 + n_3^2 = 1. \qquad (A3)$$

Matrix **B** in (A1) is Christoffel matrix rotated to the Cartesian coordinate system whose basis vectors are vectors $\mathbf{e}^{[i]}$.

Explicit expressions for elements of matrix **B** for a weakly anisotropic medium of arbitrary symmetry in terms of 21 WA parameters were introduced by Farra and Pšenčík (2003). In case of P waves, only 3 elements are needed: B_{13}, B_{23} and B_{33}. These elements depend on 15 (P-wave) WA parameters in the case of most general anisotropy. Element $B_{33}(\mathbf{n})$ represents the first-order approximation of the square of the phase velocity $\tilde{c}^2(\mathbf{n})$, in which the unit vector **n** plays the role of the phase vector.

In a monoclinic medium whose plane of symmetry coincides with the plane (x_1, x_2), the number of WA parameters specifying P-wave propagation reduces from 15 to 9. The elements B_{13}, B_{23} and B_{33} attain the following form:

$$B_{13}(\mathbf{n}) = \alpha_0^2 D^{-1}\Big(n_3^3(\eta_y n_1^2 + \eta_x n_2^2 + 2\chi_z n_1 n_2) + n_3[(2\eta_z - \eta_x - \eta_y) n_1^2 n_2^2$$

$$+2(2\epsilon_{16} - \chi_z) n_1^3 n_2 + 2(2\epsilon_{26} - \chi_z) n_1 n_2^3 - \eta_y n_1^4 - \eta_x n_2^4 + (\epsilon_x - \epsilon_z) n_1^2 + (\epsilon_y - \epsilon_z) n_2^2]\Big),$$

$$B_{23}(\mathbf{n}) = \alpha_0^2 D^{-1}\Big(n_3^2[(\eta_x - \eta_y) n_1 n_2 + \chi_z n_1^2 - \chi_z n_2^2]$$

$$+\eta_z n_1^3 n_2 - \eta_z n_1 n_2^3 + 3(\epsilon_{26} - \epsilon_{16}) n_1^2 n_2^2 + \epsilon_{16} n_1^4 - \epsilon_{26} n_2^4 + (\epsilon_y - \epsilon_x) n_1 n_2\Big),$$

$$B_{33}(\mathbf{n}) = \tilde{c}^2(\mathbf{n}) = \alpha_0^2\Big(1 + 2[n_3^2(\eta_y n_1^2 + \eta_x n_2^2 + 2\chi_z n_1 n_2 + \epsilon_z)$$

$$+\epsilon_x n_1^2 + \epsilon_y n_2^2 + \eta_z n_1^2 n_2^2 + 2\epsilon_{16} n_1^3 n_2 + 2\epsilon_{26} n_1 n_2^3]\Big). \qquad (A4)$$

The symbol α_0 in (A4) denotes the P-wave velocity in a reference (background) isotropic medium. The WA parameters used in (A4) are defined along with equation (1) in the main text. In (A4), the following variables are also used:

$$\eta_x = \delta_x - \epsilon_y - \epsilon_z, \quad \eta_y = \delta_y - \epsilon_x - \epsilon_z, \quad \eta_z = \delta_z - \epsilon_x - \epsilon_y. \qquad (A5)$$

Appendix B

Matrix **B** *and WA parameters along a profile*

Let us consider a local Cartesian coordinate system x'_i, whose x'_3-axis coincides with the x_3 axis of the global coordinate system, and both systems have a common origin. The axis x'_1 makes an (azimuth) angle φ with the x_1-axis of the global coordinate system. Transformation between the two coordinate systems is controlled by the rotation matrix:

$$\begin{pmatrix} \cos\varphi & \sin\varphi & 0 \\ -\sin\varphi & \cos\varphi & 0 \\ 0 & 0 & 1 \end{pmatrix}. \qquad (B1)$$

We use primes to denote the quantities, including the WA and the density-normalized elastic parameters, defined with respect to the local Cartesian coordinate system. The non-primed quantities are defined with respect to the global Cartesian coordinate system.

Let us consider a monoclinic medium or a medium of a higher symmetry overlaying a horizontal reflector, which coincides with a symmetry plane of the considered medium. In such a model, a ray of a reflected unconverted P wave is confined to a vertical plane and down-going and up-going rays are symmetrical with respect to the normal to the reflector. Let us consider, for example, the down-going ray and let us assume that it is situated in the vertical plane (x'_1, x'_3). The direction of the ray is specified by the unit vector $\mathbf{N} \equiv (N'_1, 0, N'_3)$ with its components expressed in the local Cartesian coordinates x'_i. The elements $B_{13}(\mathbf{N})$, $B_{23}(\mathbf{N})$ and $B_{33}(\mathbf{N}) = \tilde{c}^2(\mathbf{N})$ required in equations (6) - (8) can be determined from expressions (A1). If we consider $\alpha_0^2 = A'_{33} = A_{33}$ resulting in $\epsilon'_z = 0$ and also $D = |N'_1|$, we get from (A4):

$$B_{13}(\mathbf{N}) = \alpha_0^2 N'_1 N'_3 [\delta'_y - 2(\delta'_y - \epsilon'_x) N'^2_1],$$

$$B_{23}(\mathbf{N}) = \alpha_0^2 N'_1 (\chi'_z N'^2_3 + \epsilon'_{16} N'^2_1),$$

$$\tilde{c}^2(\mathbf{N}) = B_{33}(\mathbf{N}) = \alpha_0^2 \Big(1 + 2N'^2_1 [\epsilon'_x + (\delta'_y - \epsilon'_x) N'^2_3]\Big). \qquad (B2)$$

Monoclinic media

We can see that expressions (B2) for monoclinic media depend on 4 primed WA parameters ϵ'_x, δ'_y, χ'_z and ϵ'_{16} in the local coordinate system. They are related to 8 of 9 WA parameters in the global coordinate system (remember, $\epsilon'_z = 0$). The transformation relations read:

$$\epsilon'_x = \epsilon_x \cos^4\varphi + 2\epsilon_{16} \cos^3\varphi \sin\varphi + \delta_z \cos^2\varphi \sin^2\varphi + \epsilon_y \sin^4\varphi + 2\epsilon_{26} \cos\varphi \sin^3\varphi,$$

$$\delta'_y = \delta_y \cos^2\varphi + 2\chi_z \sin\varphi \cos\varphi + \delta_x \sin^2\varphi,$$

$$\chi'_z = \chi_z \cos 2\varphi + (\delta_x - \delta_y) \sin\varphi \cos\varphi,$$

$$\epsilon'_{16} = -2\epsilon_x \cos^3\varphi \sin\varphi + 2\epsilon_y \sin^3\varphi \cos\varphi + \delta_z \cos\varphi \sin\varphi \cos 2\varphi + \epsilon_{16} \cos^4\varphi$$
$$+3(\epsilon_{26} - \epsilon_{16}) \cos^2\varphi \sin^2\varphi - \epsilon_{26} \sin^4\varphi. \qquad (B3)$$

The above transformation relations follow from the corresponding transformation relations for parameters $A_{\alpha\beta}$ specified in the global and local Cartesian coordinate systems (note that there is a direct linear relation between WA and $A_{\alpha\beta}$ parameters).

Orthorhombic media

Let us consider an orthorhombic medium, whose symmetry planes coincide with the coordinate planes of the global coordinate system. In such a medium, we have

$$\chi_z = \epsilon_{16} = \epsilon_{26} = 0. \tag{B4}$$

This means that the number of WA parameters specifying P-wave propagation reduces from 9 to 6. If we consider, again, $\alpha_0^2 = A'_{33} = A_{33}$, and thus $\epsilon'_z = 0$, the number of WA parameters reduces to 5. The number of the primed WA parameters in the plane (x'_1, x'_3) remains 4, but the transformation relations further simplify, compared to (B3), to:

$$\begin{aligned}
\epsilon'_x &= \epsilon_x \cos^4\varphi + \delta_z \cos^2\varphi \sin^2\varphi + \epsilon_y \sin^4\varphi, \\
\delta'_y &= \delta_y \cos^2\varphi + \delta_x \sin^2\varphi, \\
\chi'_z &= (\delta_x - \delta_y) \sin\varphi \cos\varphi, \\
\epsilon'_{16} &= -2\epsilon_x \cos^3\varphi \sin\varphi + 2\epsilon_y \sin^3\varphi \cos\varphi + \delta_z \cos\varphi \sin\varphi \cos 2\varphi.
\end{aligned} \tag{B5}$$

Transversely isotropic media with horizontal axis of symmetry (HTI)

In HTI media with axis of symmetry parallel to the x_1 axis, we have, in addition to (B4):

$$\epsilon_y = \epsilon_z = \frac{1}{2}\delta_x, \quad \delta_y = \delta_z. \tag{B6}$$

The number of WA parameters specifying P-wave propagation reduces from 6 to 3. For $\alpha_0^2 = A'_{33} = A_{33}$ ($\epsilon'_z = 0$), the number of WA parameters reduces to 2. The number of the primed WA parameters in the plane (x'_1, x'_3) remains 4, but the transformation relations further simplify to:

$$\begin{aligned}
\epsilon'_x &= \epsilon_x \cos^4\varphi + \delta_y \cos^2\varphi \sin^2\varphi, \\
\delta'_y &= \delta_y \cos^2\varphi, \\
\chi'_z &= -\delta_y \sin\varphi \cos\varphi, \\
\epsilon'_{16} &= -2\epsilon_x \cos^3\varphi \sin\varphi + \delta_y \cos\varphi \sin\varphi \cos 2\varphi.
\end{aligned} \tag{B7}$$

Transversely isotropic media with vertical axis of symmetry (VTI)

For completeness, we present here also transformation relations for VTI media. In VTI media, we have, in addition to (B4):

$$\epsilon_x = \epsilon_y = \frac{1}{2}\delta_z, \quad \delta_x = \delta_y. \tag{B8}$$

The number of WA parameters specifying P-wave propagation is 3 as in the HTI case. For $\alpha_0^2 = A'_{33} = A_{33}$, and thus $\epsilon'_z = 0$, the number of WA parameters reduces again to 2. The number of the primed WA parameters in the plane (x'_1, x'_3) reduces to two in the VTI case:

$$\epsilon'_x = \epsilon_x, \qquad \delta'_y = \delta_y, \qquad \chi'_z = \epsilon'_{16} = 0. \tag{B9}$$

The primed WA parameters ϵ'_x, δ'_y are equal to the WA parameters ϵ_x, δ_y in the global Cartesian coordinate system.

Appendix C

Moveout coefficients

Because we do not use Taylor expansion of traveltime for the derivation of moveout formulae, in principle, we do not need quadratic and quartic coefficients of the Taylor expansion that occur in the expressions for T^2 published in literature (Taner and Koehler, 1969; Tsvankin and Grechka, 2011, etc.). They are, however, useful for the comparison of our formulae with formulae based on the Taylor expansion. Additionally, they also offer one possible way of extension of our formulae to media composed of a set of horizontal layers.

Let us first consider the Taylor expansion of T^2 with respect to x^2 along a selected profile. Along it, we have:

$$T^2 = A_0 + A_2 x^2 + A_4 x^4 + ..., \tag{C1}$$

where A_i coefficients contain derivatives of the squared traveltime with respect to the squared offset x^2. The coefficient A_0 represents the square of the two-way zero-offset traveltime T_0:

$$A_0 = T_0^2 \ . \tag{C2}$$

The coefficient A_2 represents the inverse of the square of the NMO velocity v_{NMO}:

$$A_2 = v_{NMO}^{-2} \ . \tag{C3}$$

By differentiating the traveltime expressions (12), (16) and (20) with respect to the square of offset x^2 and taking into account the relation between offset x and normalized offset $\bar{x}$, see equation (3), we can evaluate the coefficients A_i, for $i = 1$ and 2 with the accuracy determined by the used traveltime formula. The coefficient A_0 is in all cases given by (C2).

By differentiating equation (12), we obtain

$$A_2 = (1 - 2\delta'_y)/\alpha_0^2 \tag{C4}$$

and

$$A_4 = 2[\delta'_y - \epsilon'_x + 2(\delta'_y)^2]/\alpha_0^4 T_0^2 \ . \tag{C5}$$

From eqs (C3) and (C4), we obtain

$$v_{NMO}^{-2} = (1 - 2\delta'_y)/\alpha_0^2 \ . \tag{C6}$$

Equation (C6) gives the first-order approximation of the inverse of the square of NMO velocity in monoclinic media for the case that the difference between vectors **n** and **N** is ignored. Equation (C6) coincides with eq.(41) of Pšenčík and Gajewski (1998) and corresponds, within the first order, to the first-order expression for NMO velocity given in eq.(8) of Rasolofosaon (2000). From (C6), we can see that the NMO velocity is varying with azimuth. For monoclinic media, the variation is described by the dependence of the primed WA parameter δ'_y on the WA parameters δ_x, δ_y and χ_z, see equation (B3). For orthorhombic media, the variation of v_{NMO} with azimuth is described by the dependence of δ'_y on δ_x and δ_y, see equation (B5), and for HTI media by the dependence of δ'_y on δ_y,

see (B7). From (B9), we can also see that, as expected, v_{NMO} does not depend on the azimuth in VTI media.

Equation (C5) with ϵ'_x and δ'_y expressed through (B3), (B5) or (B7) yields the azimuthal dependence of the quartic coefficient A_4 in monoclinic, orthorhombic or HTI medium. Using (B9) in (C5), we can see that, as expected, the quartic coefficient A_4 in VTI media does not depend on azimuth and, if we neglect the quadratic terms, (C5) is equivalent to the expression (3.6) of Tsvankin and Grechka (2011) specified for $F = 1$.

Alternatively, by differentiating equation (16), we obtain

$$A_2 = [1 - 2\delta'_y + 4\Big((\delta'_y)^2 + (\chi'_z)^2\Big)]/\alpha_0^2 \qquad (C7)$$

and

$$A_4 = \Big(2[\delta'_y - \epsilon'_x + 2(\delta'_y)^2] - 4[5(\delta'_y)^2 - 4\epsilon'_x\delta'_y + 2\chi'_z(\chi'_z - \epsilon'_{16})]\Big)/\alpha_0^4 T_0^2 \ . \qquad (C8)$$

From (C3) and (C7), we get

$$v_{NMO}^{-2} = [1 - 2\delta'_y + 4\Big((\delta'_y)^2 + (\chi'_z)^2\Big)]/\alpha_0^2 \ . \qquad (C9)$$

This is again the first-order NMO velocity, but in this case, the difference between the vectors $\mathbf{n}$ and $\mathbf{N}$ is considered, resulting in a more accurate expression for v_{NMO}. Its azimuthal dependence is more complicated than in equation (C6) because NMO velocity depends on the additional primed WA parameter χ'_z.

Finally, if we differentiate equation (20), we obtain

$$A_2 = [1 - 2\delta'_y - 4a\Big((\delta'_y)^2 + (\chi'_z)^2\Big)]/\alpha_0^2 \qquad (C10)$$

and

$$A_4 = \Big(2[\delta'_y - \epsilon'_x + 2(\delta'_y)^2] + 4a[5(\delta'_y)^2 - 4\epsilon'_x\delta'_y + 2\chi'_z(\chi'_z - \epsilon'_{16})]\Big)/\alpha_0^4 T_0^2 \ , \qquad (C11)$$

where $a = (r^2 - 3/4)/(1 - r^2)$ and $r = \beta_0/\alpha_0$.

When deriving equation (C11), we neglected all the terms of order higher than 2 in WA parameters. Equations (C3) and (C10) yield the second-order approximation for the inverse square of the NMO velocity

$$v_{NMO}^{-2} = [1 - 2\delta'_y - 4a\Big((\delta'_y)^2 + (\chi'_z)^2\Big)]/\alpha_0^2 \ . \qquad (C12)$$

All the above expressions are specified with respect to a selected profile. In order to get expressions describing azimuthal variation of coefficients A_2 and A_4, we do not need to derive and linearize complicated exact expression, see Al Dajani et al. (1998). It is sufficient to express the primed WA parameters in equations (C4)-(C12) in terms of "global" WA parameters (1), using transformation relations of Appendix B. We will show that in such cases the v_{NMO} formulae above attain the well-known form of azimuthally-varying v_{NMO} introduced by Grechka and Tsvankin (1998):

$$v_{NMO}^{-2}(\varphi) = W_{11}\cos^2\varphi + 2W_{12}\cos\varphi\sin\varphi + W_{22}\sin^2\varphi \ . \qquad (C13)$$

In equation (C13), angle φ is the azimuth measured from the x_1-axis of the global coordinate system towards the x_2-axis.

First, if we insert δ'_y from (B3) to equation (C6), we can rewrite equation (C6) to the form (C13), with coefficients W_{IJ}:

$$W_{11} = \alpha_0^{-2}(1 - 2\delta_y) \ , \quad W_{12} = -2\alpha_0^{-2}\chi_z \ , \quad W_{22} = \alpha_0^{-2}(1 - 2\delta_x) \ . \qquad (C14)$$

This is also identical to equation (43) of Pšenčík and Gajewski (1998) and equal, to the first order, to equations (8) and (B-1) of Rasolofosaon (2000). Approximation (C14) is of the first order and holds, as shown in the above references, for an arbitrary anisotropic symmetry.

Second, if we insert expressions (B3) for δ'_y and χ'_z to equation (C12), we obtain, again, (C13) with coefficients W_{IJ}:

$$W_{11} = \alpha_0^{-2}[1 - 2\delta_y - 4a(\delta_y^2 + \chi_z^2)] \ , \quad W_{12} = -2\alpha_0^{-2}\chi_z[1 + 2a(\delta_x + \delta_y)] \ ,$$

$$W_{22} = \alpha_0^{-2}[1 - 2\delta_x - 4a(\delta_x^2 + \chi_z^2)] \ . \qquad (C15)$$

Now, equation (C13) with coefficients (C15) represents azimuthally varying second-order approximation of the NMO velocity for a monoclinic layer. Coefficients (C15) represent the second-order approximations of the exact coefficients derived by Grechka et al. (2000). They thus give a better approximation than the coefficients given in equation (26) of Grechka et al. (2000), which are of the first order.

The coefficients (C15) of the second-order approximation of the NMO velocity for a monoclinic medium depend on three WA parameters, δ_x, δ_y and χ_z. In orthorhombic media, with the vertical symmetry planes coinciding with the coordinate planes (equation B4), using transformations (B5), coefficients (C14) and (C15) reduce to:

$$W_{11} = \alpha_0^{-2}(1 - 2\delta_y) \ , \quad W_{12} = 0 \ , \quad W_{22} = \alpha_0^{-2}(1 - 2\delta_x) \qquad (C16)$$

or

$$W_{11} = \alpha_0^{-2}[1 - 2\delta_y(1 + 2a\delta_y)] \ , \quad W_{12} = 0 \ , \quad W_{22} = \alpha_0^{-2}[1 - 2\delta_x(1 + 2a\delta_x)] \ , \qquad (C17)$$

respectively. The coefficients of the second-order approximation of the NMO velocity (C17) thus depend on only two WA parameters δ_x and δ_y. The NMO-velocity formula simplifies further for HTI media. For the specification (B6), i.e., for the axis of symmetry parallel to the x_1-axis, equations (C16) yield:

$$W_{11} = \alpha_0^{-2}(1 - 2\delta_y) \ , \quad W_{12} = 0 \ , \quad W_{22} = \alpha_0^{-2} \qquad (C18)$$

and equations (C17) yield:

$$W_{11} = \alpha_0^{-2}[1 - 2\delta_y(1 + 2a\delta_y)] \ , \quad W_{12} = 0 \ , \quad W_{22} = \alpha_0^{-2} \ . \qquad (C19)$$

Finally, in a VTI medium, using the specification (B8), we obtain from equation (C16):

$$W_{11} = W_{22} = \alpha_0^{-2}(1 - 2\delta_y) \ , \quad W_{12} = 0 \qquad (C20)$$

and from equation (C17):

$$W_{11} = W_{22} = \alpha_0^{-2}[1 - 2\delta_y(1 + 2a\delta_y)] \ , \quad W_{12} = 0 \ . \tag{C21}$$

As expected, equations (C20) and (C21) confirm axial symmetry of the NMO velocity in VTI media. Equation (C21) has been previously obtained by Farra and Pšenčík (2013a).

Applying the same transformation process as for the NMO velocity, we can also express quartic coefficients A_4 as functions of azimuth. Starting with the least accurate approximation (C5), applying transformations (B3) we arrive at

$$\begin{aligned} A_4(\varphi) = A_4^{(1)} \sin^2\varphi + A_4^{(2)} \cos^2\varphi + A_4^{(x)} \sin^2\varphi \cos^2\varphi \\ + A_4^{(x2)} \sin\varphi \cos^3\varphi + A_4^{(x3)} \sin^3\varphi \cos\varphi \ . \end{aligned} \tag{C22}$$

In (C22),

$$A_4^{(1)} = -\frac{2}{\alpha_0^4 T_0^2}(\epsilon_y - \delta_x - 2\delta_x^2) \ , \quad A_4^{(2)} = -\frac{2}{\alpha_0^4 T_0^2}(\epsilon_x - \delta_y - 2\delta_y^2) \ ,$$

$$A_4^{(x)} = \frac{2}{\alpha_0^4 T_0^2}[\epsilon_x + \epsilon_y - \delta_z - 2(\delta_x - \delta_y)^2 + 8\chi_z^2] \ ,$$

$$A_4^{(x2)} = -\frac{4}{\alpha_0^4 T_0^2}(\epsilon_{16} - \chi_z - 4\delta_y\chi_z) \ , \quad A_4^{(x3)} = -\frac{4}{\alpha_0^4 T_0^2}(\epsilon_{26} - \chi_z - 4\delta_x\chi_z) \ . \tag{C23}$$

The approximation (C22) is consistent with the result by Al-Dajani et al. (1998), see their equation (4) for $A_4(\varphi)$. Relatively simple expressions (C22) and (C23) for the quartic coefficient in monoclinic media were obtained under the assumption of weak anisotropy only. No assumption of zero shear-wave velocity, employed by Al-Dajani et al. (1998), was used in the derivation here.

In a medium of orthorhombic symmetry, whose planes of symmetry coincide with the coordinate planes of the global Cartesian coordinate system (ϵ_{16}, ϵ_{26} and χ_z are zero), equations (C22) and (C23) yield a slightly modified form of eq.(6) of Al-Dajani et al. (1998):

$$A_4(\varphi) = A_4^{(1)} \sin^2\varphi + A_4^{(x)} \sin^2\varphi \cos^2\varphi + A_4^{(2)} \cos^2\varphi \tag{C24}$$

with coefficients

$$A_4^{(1)} = -\frac{2}{\alpha_0^4 T_0^2}(\epsilon_y - \delta_x - 2\delta_x^2) \ , \quad A_4^{(2)} = -\frac{2}{\alpha_0^4 T_0^2}(\epsilon_x - \delta_y - 2\delta_y^2) \ ,$$

$$A_4^{(x)} = \frac{2}{\alpha_0^4 T_0^2}[\epsilon_x + \epsilon_y - \delta_z - 2(\delta_x - \delta_y)^2] \ . \tag{C25}$$

Coefficients (C25) are first-order approximations (in which the difference between the phase and ray vectors $\mathbf{n}$ and $\mathbf{N}$ is neglected) of coefficients (10) and (11) of Al Dajani et al. (1998). If we neglect the second-order terms in (C25), we can see that the coefficients $A_4^{(1)}$ and $A_4^{(2)}$ are equivalent to the corresponding coefficients in equation (3.25) of Tsvankin and Grechka (2011). The same also holds for the coefficient $A_4^{(x)}$, taking into account the differences in the notation in Tsvankin and Grechka (2011) and here.

Let us emphasize several important facts. For the derivation of coefficients (C25), no acoustic approximation (Alkhalifah, 2000a) was used. Equations (C24) and (C25), which exactly compare to previously published formulae in literature, represent the least accurate approximation of the quartic coefficient of nonhyperbolic moveout (see Figure 5). Using our approach, the accuracy can be easily further improved starting with more accurate equations (C8) or (C11) instead of (C5). It should also be mentioned that, in contrast to nonhyperbolic moveout formula of Tsvankin and Thomsen (1994), the Taylor expansion (C1) with coefficients (C2), (C4), (C7) or (C10) and (C5), (C8) or (C11) requires no correction for convergency of the traveltime formula for large offsets.

References

Al-Dajani, A., I. Tsvankin, and M. N. Toksöz, 1998, Nonhyperbolic reflection moveout for azimuthally anisotropic media: 68th Ann. Internat. Mtg., Soc. Expl. Geophys., Expanded Abstracts, 1479-1482.

Alkhalifah, T., 2000a, An acoustic wave equation for anisotropic media: Geophysics, **65**, 1239–1250.

Alkhalifah, T., 2000b, The offset-midpoint traveltime pyramide for transversely isotropic media: Geophysics, **65**, 1316–1325.

Alkhalifah, T., and I. Tsvankin, 1995, Velocity analysis for transversely isotropic media: Geophysics, **60**, 1550–1566.

Bakker, P., 2002, Coupled anisotropic shear-wave ray tracing in situations where associated slowness sheets are almost tangent: Pure appl. Geophys., **159**, 1403-1417.

Chen, M., and J. Tromp, 2007, Theoretical and numerical investigations of global and regional seismic wave propagation in weakly anisotropic earth models: Geophys. J. Int., **168**, 1130-1152.

Farra, V., and I. Pšenčík, 2003, Properties of the zero-, first- and higher-order approximations of attributes of elastic waves in weakly anisotropic media: J. Acoust. Soc. Am., **114**, 1366–1378.

Farra, V., and I. Pšenčík, 2008, First-order ray computations of coupled S waves in inhomogeneous weakly anisotropic media: Geophys. J. Int., **173**, 979-989.

Farra, V., and I. Pšenčík, 2010, Coupled S waves in inhomogeneous weakly anisotropic media using first-order ray tracing: Geophys. J. Int., **180**, 405-417.

Farra, V., and I. Pšenčík, 2013a, Moveout approximations for P and SV waves in VTI media: Geophysics, **78**, WC81–WC92.

Farra, V., and I. Pšenčík, 2013b, Moveout approximations for P and SV waves in dip-constrained transversely isotropic media: Geophysics, **78**, C53–C59.

Farra, V., and I. Pšenčík, 2014, Moveout approximations for P waves in media of

monoclinic and higher anisotropy symmetries: Seismic Waves in Complex 3-D Structures, **24**, 35–58, online at "http://sw3d.cz".

Fomel, S., 2004, On anelliptic approximations for qP velocities in VTI media: Geophys. Prosp., **52**, 247–259.

Fomel, S., 2014. Recent advances in time-domain seismic imaging: 84th Ann. Internat. Mtg., Soc. Expl. Geophys., Expanded Abstracts, 4400–4404.

Gajewski, D., and I. Pšenčík, 1990, Vertical seismic profile synthetics by dynamic ray tracing in laterally varying layered anisotropic structures: J. Geophys. Res., **95**, 11301–11315.

Grechka, V., P. Contreras, and I. Tsvankin, 2000, Inversion of normal moveout for monoclinic media: Geophys. Prosp., **48**, 577–602.

Grechka, V., and I. Tsvankin, 1998, 3-D description of normal moveout in anisotropic inhomogeneous media: Geophysics, **63**, 1079–1092.

Klimeš, L., 2006, Common-ray tracing and dynamic ray tracing for S waves in a smooth elastic anisotropic medium: Stud. Geophys. Geod., **50**, 449-461.

Li, S., and S. Fomel, 2013. A robust approach to time-to-depth conversion in the presence of lateral-velocity variations: 83rd Ann. Internat. Mtg., Soc. Expl. Geophys., Expanded Abstracts, 4800–4805.

Mensch, T., and P. Rasolofosaon, 1997, Elastic-wave velocities in anisotropic media of arbitrary symmetry – generalization of Thomsens parameters ϵ, δ and γ: Geophys. J. Int., **128**, 43–64.

Pšenčík, I., and D. Gajewski, 1998, Polarization, phase velocity and NMO velocity of qP waves in arbitrary weakly anisotropic media: Geophysics, **63**, 1754–1766.

Pšenčík, I., and V. Farra, 2005, First-order ray tracing for qP waves in inhomogeneous weakly anisotropic media: Geophysics, **70**, D65–D75.

Pšenčík, I., and V. Farra, 2007, First-order P-wave ray synthetic seismograms in inhomogeneous weakly anisotropic media: Geophys.J.Int., **170**, 1243–1252.

Rasolofosaon, P., 2000, Explicit analytic expression for normal moveout from horizontal and dipping reflectors in weakly anisotropic media of arbitrary symmetry type: Geophysics, **65**, 1294-1304.

Růžek, B., and I. Pšenčík, 2014, P-wave traveltime inversion in weakly anisotropic media: a preliminary study: Seismic Waves in Complex 3-D Structures, **24**, 17–34, online at "http://sw3d.cz".

Sayers, C. M., and D. A. Ebrom, 1997, Seismic traveltime analysis for azimuthally anisotropic media: Theory and experiment: Geophysics, **62**, 1570-1582.

Schoenberg, M., and K. Helbig, 1997, Orthorhombic media: Modeling elastic wave behavior in a vertically fractured earth: Geophysics, **62**, 1954–1974.

Schoenberg, M., and C. Sayers, 1995, Seismic anisotropy of fractured rock: Geophysics,

60, 204–211.

Stovas, A., 2010, Generalized moveout approximation for qP- and qSV-waves in a homogeneous transversely isotropic medium: Geophysics, **75**, D79–D84.

Taner, M. T., and F. Koehler, 1969, Velocity spectra digital computer derivation and applications of velocity functions: Geophysics, **34**, 859-881.

Thomsen, L., 1986, Weak elastic anisotropy: Geophysics, **51**, 1954–1966.

Tsvankin, I., 1997, Anisotropic parameters and P-wave velocity for orthorhombic media: Geophysics, **62**, 1292-1309.

Tsvankin, I., 2001, Seismic signatures and analysis of reflection data in anisotropic media: Oxford, Elsevier Science Ltd.

Tsvankin, I., and V. Grechka, 2011, Seismology of azimuthally anisotropic media and seismic fracture characterization: Society of Exploration Geophysicists.

Tsvankin, I., and L. Thomsen, 1994, Nonhyperbolic reflection moveout in anisotropic media: Geophysics, **59**, 1290-1304.

Ursin, B., and A. Stovas, 2006, Traveltime approximations for a layered transversely isotropic medium: Geophysics, **71**, D23-D33.